

Development of a Design Guide for Ultra Thin Whitetopping (UTW)

FINAL REPORT
November 1998

Submitted by
Nenad Gucunski
Professor

Center for Advanced Infrastructure & Transportation (CAIT)
Civil & Environmental Engineering
Rutgers, The State University
Piscataway, NJ 08854-8014



NJDOT Research Project Manager
Mr. Nicholas Vitillo

In cooperation with

New Jersey
Department of Transportation
Division of Research and Technology
and
U.S. Department of Transportation
Federal Highway Administration

Disclaimer Statement

"The contents of this report reflect the views of the author(s) who is (are) responsible for the facts and the accuracy of the data presented herein. The contents do not necessarily reflect the official views or policies of the New Jersey Department of Transportation or the Federal Highway Administration. This report does not constitute a standard, specification, or regulation."

The contents of this report reflect the views of the authors, who are responsible for the facts and the accuracy of the information presented herein. This document is disseminated under the sponsorship of the Department of Transportation, University Transportation Centers Program, in the interest of information exchange. The U.S. Government assumes no liability for the contents or use thereof.

1. Report No. FHWA 2001 - 018		2. Government Accession No.		3. Recipient's Catalog No.	
4. Title and Subtitle Development of a Design Guide for Ultra Thin Whitetopping (UTW)				5. Report Date November 1998	
				6. Performing Organization Code CAIT/Rutgers	
7. Author(s) Dr. Nenad Gucunski				8. Performing Organization Report No. FHWA 2001 - 018	
9. Performing Organization Name and Address New Jersey Department of Transportation CN 600 Trenton, NJ 08625				10. Work Unit No.	
				11. Contract or Grant No.	
12. Sponsoring Agency Name and Address Federal Highway Administration U.S. Department of Transportation Washington, D.C.				13. Type of Report and Period Covered Final Report 03/06/1996 - 03/31/1999	
				14. Sponsoring Agency Code	
15. Supplementary Notes					
16. Abstract <p>Concrete overlay of deteriorated asphalt pavements (whitetopping) has been a viable alternative to improve the pavement's structural integrity for over six decades. The thickness of such overlay usually exceeds five inches. In the last few years, however, a newer technology has emerged which is commonly known as Ultra Thin Whitetopping (UTW). UTW is a construction technique, which involves placement of a thinner (than normal) thickness ranging from 2 to 4 inches. The application of UTW has been targeted to restore/rehabilitate deteriorated asphalt pavements with fatigue and/or rutting distress.</p> <p>Study of UTW was initiated by the construction of the first experimental project on an access road to a landfill in Louisville, Kentucky in 1991. This rather successful project was complemented by a series of experimental projects by many state and local agencies. There have been more than 170 UTW projects constructed from the early 1990's and many investigators published papers/articles on the performance of these experimental projects. As a natural outcome of experimental observations, a need for a thorough and comprehensive (theoretical) understanding of UTW system is felt amongst researchers and experimentalists. In order to gain an insight into the contribution of the many variables in a UTW pavements system (i.e., thickness of UTW, AC and baselayers; stiffness moduli of UTW, AC and base layers; size of UTW panels; UTW-AC interface; load transfer; etc.), there have been a few research endeavors.</p> <p>The intent of this research study is to identify and address important factors that contribute to the performance of the UTW pavement system. It is also the goal of this research to present an interim design procedure fine tuned by further observation of UTW pavement systems.</p>					
17. Key Words ultra thin whitetopping, UTW, concrete overlay, deteriorated asphalt, restore, rehabilitate, fatigue, rutting			18. Distribution Statement		
19. Security Classif (of this report) Unclassified		20. Security Classif. (of this page) Unclassified		21. No of Pages 54	22. Price

ACKNOWLEDGMENT

This work was supported by the New Jersey Department of Transportation and New Jersey Concrete and Aggregate Association through the Center for Advanced Infrastructure and Transportation of Rutgers University. The technical assistance and funding support by the organizations are gratefully acknowledged. SWK-Pavement Engineering, Princeton, New Jersey, was a subcontractor on the project, conducting field testing and developing the design procedure, and contributing to other phases of the project. In particular, appreciation is extended to Drs. Kaz Tabrizi and Vahid Ganji of SWK-PE for this effort. Special thanks are extended to Mr. Nick Vitillo of NJDOT and Dr. Ali Maher of Rutgers University for their advice and effort in the development of the design guide.

DEVELOPMENT OF A DESIGN GUIDE FOR ULTRA THIN WHITETOPPING (UTW)

	<u>Page Number</u>
Chapter 1 – Introduction	1
Chapter 2 – Field Testing of Route I-295 Ramp	3
NDT	3
Dynamic Cone Penetrometer	5
Visual Survey	6
ARAN	7
Pavement Coring	7
Chapter 3 – Finite Element Analysis and Verification.....	9
FEM Description	9
Parametric Study	11
FEM Verification	14
Chapter 4 - Design Procedure	16
Stress Due to Load	16
Stress Due to Temperature	18
Design Stresses	19
Fatigue Criterion	20
Traffic Data	21
Safety Factor	22
Design Procedure	22
Design Example	24
I-295 Ramp	26
Appendix A: The Heavy (Falling) Weight Deflectometer	
Appendix B: I-295 Ramp UTW Specification	
Appendix C: Back-Analyzed Deflection Data (Heavy Weight Deflectometer)	
Appendix D: Back-Analyzed Deflection Data (Falling Weight Deflectometer)	
Appendix E: Description of Dynamic Cone Penetrometer (DCP)	
Appendix F: CBR Results From DCP	
Appendix G: Prediction Equation Verification	

CHAPTER 1

Introduction

Concrete overlay of deteriorated asphalt pavements (whitetopping) has been a viable alternative to improve the pavement's structural integrity for over six decades. The thickness of such overlay usually exceeds five (5) inches. In the last few years, however, a newer technology has emerged which is commonly known as Ultra Thin Whitetopping (UTW). UTW is a construction technique, which involves placement of a thinner (than normal) thickness ranging from 2 to 4 inches. The application of UTW has been targeted to restore/rehabilitate deteriorated asphalt pavements with fatigue and/or rutting distresses.

Study of UTW was initiated by the construction of the first experimental project on an access road to a landfill in Louisville, Kentucky in 1991¹. This rather successful project was complemented by a series of experimental projects by many state and local agencies. There have been more than 170 UTW projects constructed from the early 1990s (Figure 1) and many investigators published papers/articles on the performance of these experimental projects^{2,3,4,5}. As a natural outcome of experimental observations, a need for a thorough and comprehensive (theoretical) understanding of UTW system is felt amongst researchers and experimentalists⁶. In order to gain an insight into the contribution of the many variables in a UTW pavement system (i.e., thickness of UTW, AC and base layers; stiffness moduli of UTW, AC and base layers; size of the UTW panels; UTW-AC interface; load transfer; etc.), there have been a few research endeavors⁷.

The intent of this research study is to identify and address important factors that contribute to the performance of the UTW pavement system. It is also the goal of this research to present an interim design procedure fine tuned by further observation of UTW pavement systems.

This report is divided into four chapters. Chapter 2 illustrates the field testing of a UTW ramp constructed in 1994 in New Jersey, using Heavy Weight Deflectometer (HWD), Falling Weight Deflectometer (FWD), Dynamic Cone Penetrometer (DCP), visual survey and pavement cores. The performance of a UTW pavement system is studied using a 3-Dimensional Finite Element Model (FEM). Chapter 3 provides an in-depth look at the FEM and its simulation of traffic loading, UTW, AC and base layer thicknesses; UTW-AC interface and its influence on the performance of the pavement system. Finally, Chapter 4 presents an interim design procedure based on the experiences gained from field testing and the Finite Element Model. A hypothetical design example is also presented in this chapter.

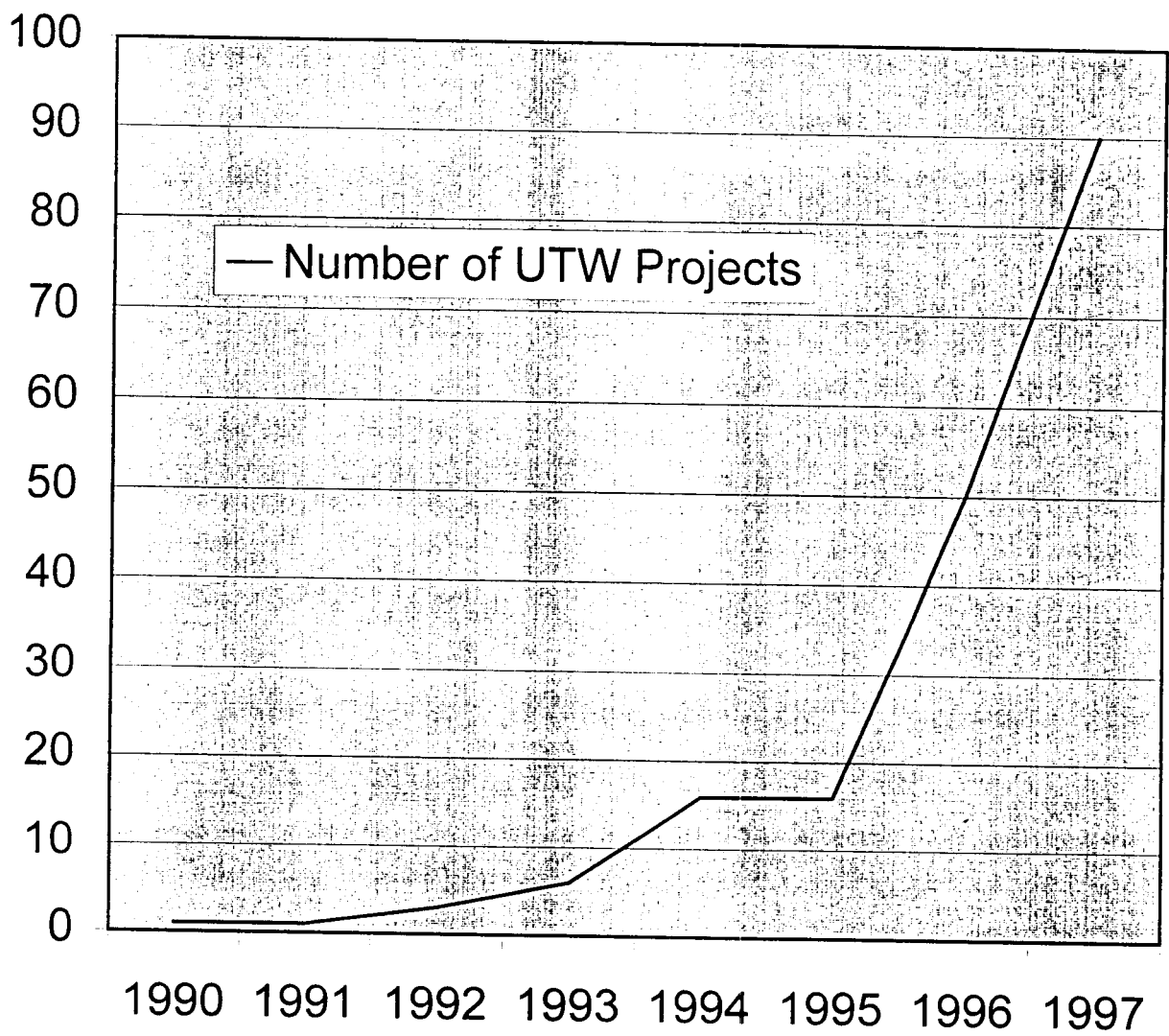


Figure 1.1: Growth of UTW Projects

CHAPTER 2

Field Testing on Route I-295 Ramp

In the month of August 1994, New Jersey Department of Transportation (NJDOT) programmed construction of a UTW on an existing bituminous ramp connecting Route I-295 Northbound to Route 130 Northbound (Figure 2). This was achieved by milling the distressed bituminous surface, an average of three (3) inches prior to the placement of UTW. Due to the geometric limitations, UTW was placed in two 9-ft. wide segments with a joint separating them. As an experimental project, NJDOT sought to evaluate the performance of three different panel sizes. The panel sizes were 3' by 3'; 4' by 4'; and 6' by 6'. The specification used with this construction is presented in Appendix B.

In the month of July 1997, SWK Pavement Engineering, Inc. (SWKPE) was commissioned to manage the field testing as part of the research on developing a design guide for UTW. In coordination with the Research and Geotechnical Engineering Bureaus of NJDOT the following were utilized:

Non-Destructive Testing: Heavy Weight Deflectometer (HWD) and Falling Weight Deflectometer (FWD)

HWD and FWD were utilized to determine the in-situ stiffness of the UTW, AC base and granular bases. Testing across the sawed joints (between the panels) also allowed for determination and ranking of their load transfer efficiency.

Reference is made to Appendix "A" for general description of both HWD/FWD. Back-calculation analyses of the deflection data for HWD testing (conducted by SWKPE) yielded reasonable results where those for FWD testing (conducted by others) did not. It is believed that the main reason for the successful results using HWD lies in the geophone re-configuration prior to field testing. Due to the limited width (or length) of

the UTW panels, HWD geophones were reconfigured according to Figure 3. Using this reconfiguration, the maximum number of geophones were utilized in 3' by 3' and 4' by 4' slabs and therefore, the stiffnesses of the layers could be determined. For example, for a 3' by 3' slab, d_1 , d_2 , d_3 , d_4 and d_{4a} were used.

Non-destructive testing was performed on a total of 45 locations which consisted of: 29 locations on 3' by 3' panels, 10 locations on 4' by 4' panels, and 6 locations on 6' by 6' panels.

Back analyzed deflection data for HWD testing (by SWK) is presented in Appendix C and that for FWD in Appendix D. Deflection data was analyzed in order to determine the in-situ layer stiffnesses and load transfer capability of the saw cut joints.

Statistical analysis of HWD back-calculated data yields similar UTW stiffness for both 3' and 4' slabs (32000 Mpa and 35000 Mpa, respectively) but the analysis for the 6' slabs resulted in almost half the above stiffness (i.e., 18000 Mpa). Analyzing the back-calculated data for AC layer reveals that the temperature adjusted stiffnesses for 3, 4 and 6 feet slab sizes are 1900 Mpa, 1100 Mpa and 1900 Mpa, respectively. It may be concluded that the in-situ stiffnesses of bituminous base material are below the normal range of 1500 – 3500 Mpa⁸.

To determine and rank load transfer across joints, the criteria indicated in Table 2.1 below were utilized. Referring to Appendix C, it is observed that the majority of joints exhibit satisfactory condition.

Table 2.1: Criteria for Ranking Joints

Deflection criteria	A	B	C	D
Load Transfer, $\delta_{.12}/\delta_0(\%)$	>75.0	60.0 - 74.9	50.0 - 59.9	<49.9
Load Transfer, $\delta_0 - \delta_{.12}$ (Microns, normalized to 700 kPa)	>50.0	50.1 - 75.0	75.1 - 100.0	<100.1
Slab (Leave) Rotation (degrees/1000 normalized to 700 kPa)	>10.0	10.1 - 15.0	15.1 - 20.0	<20.1
Intercept at zero load (microns)	>50.0	>50.0	<50.0	<50.0

Dynamic Cone Penetrameter (DCP):

DCP testing was performed to obtain a continuous reading of California Bearing Ratio (CBR) with depth. A description of the instrument and the method of use can be found with graphical results of the testing in Appendix “E”. The thickness of the granular base was used in the back-calculation of the HWD deflection data for determination of the layer stiffnesses.

The DCP survey consisted of 3 tests, performed in each core hole. The DCP test numbers correspond to the core numbers (i.e., DCP test 4.14 is located at Core 4.14). The detailed result of each DCP test is presented in Appendix “F”. The CBR values summarized in Table 2 are the in-situ CBR values obtained in the field.

Table 2.2: CBR of Dense Graded Base Course below AC

Location	Grid Size	Avg. CBR Values
3.9	3' X 3'	60
4.11	4' X 4'	55
4.14	4' X 4'	40 for top 7 inches
		85 for the rest

Visual Survey:

A visual survey of the ramp was carried out in order to determine the areas of significant distress. Certain panels were marked for coring. The survey is conducted at walking speed with distresses logged for each pavement area. The scope of the survey included noting the distresses for each slab.

The survey revealed that the major forms of visual distress for the pavement structure are cracking and corner breaking. The majority of these distresses have been observed to be concentrated in the area of the construction joint. The construction joint was formed in the centerline of the ramp during construction for practical purposes. Although the distresses appear to be severe in certain areas, except in one or two cases (in 6' by 6' slabs) the pieces are tightly in place. Particular comments for each slab sizes are as follows:

3' by 3' slabs:

3' by 3' slabs have performed the best when compared with other sizes. Areas of major distresses are in a stretch of 30 feet, 180 feet from the start of the ramp from I-295. Random distresses are also observed but are scattered.

4' by 4' slabs:

These slabs start approximately 320 feet from Route I-295 where the 3' by 3' slabs end. They are more distressed than 3' by 3' slabs and the distresses are concentrated in the vicinity of the construction joint in the middle of the ramp. The areas of best performance, measured from I-295, are from 320' to 350', 494' to 534', and 590' to 634' where 6' by 6' slabs begin.

6' by 6' slabs

The slabs in this area appeared to be in worse condition than other slab sizes. Cracking and corner breaks, however, are concentrated in the vicinity of the construction joint. It is to be noted that during the planning stage of the construction, the 6' slabs were predicted to be the worst performing of all slabs.

ARAN:

During the field investigation of the I-295 ramp, New Jersey Department of Transportation employed "ARAN" equipment for automatic (video) survey of the pavement and measurement of its roughness. The data obtained was not available and may be used in conjunction with other findings in the field in the future.

Pavement Coring:

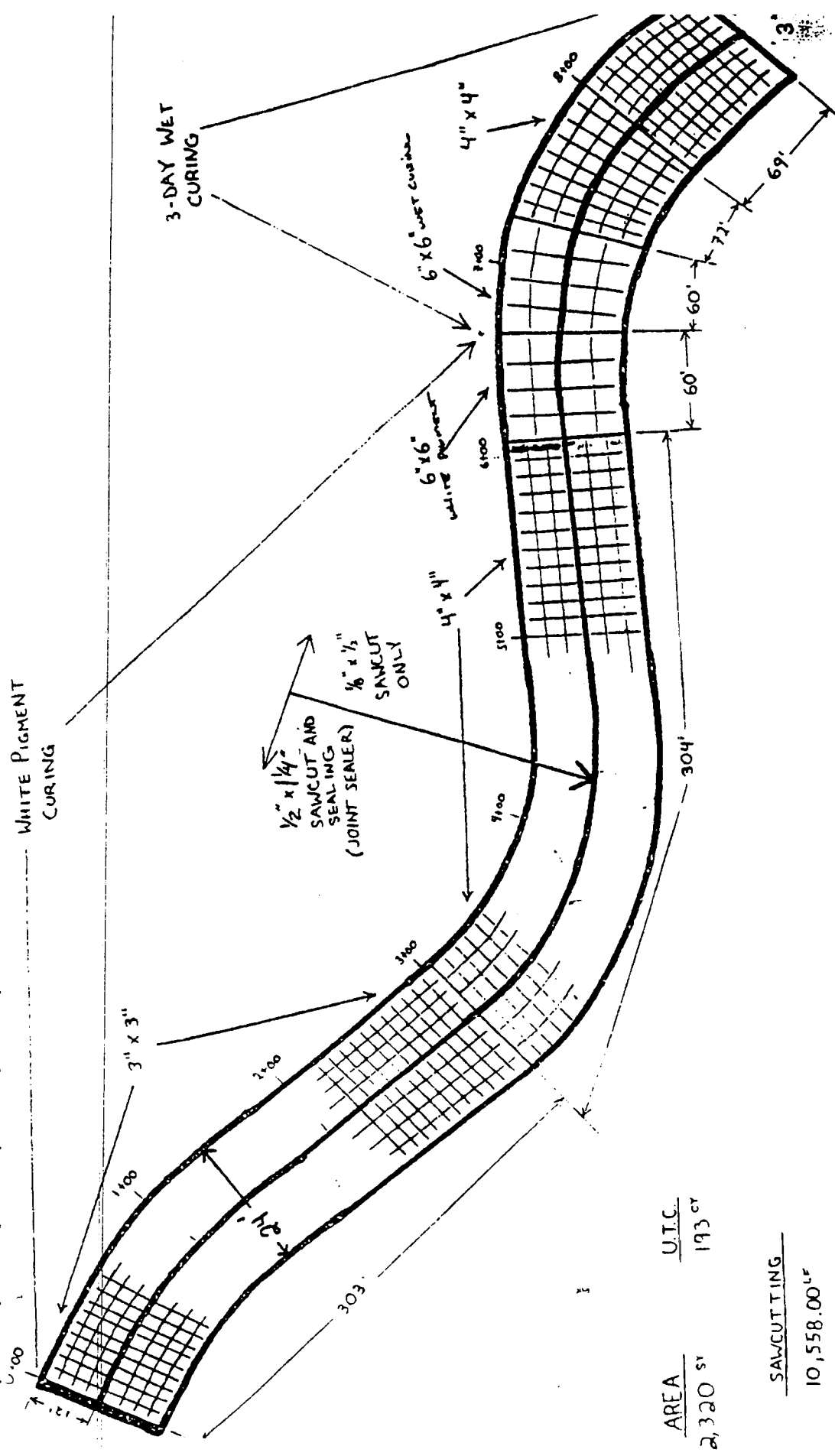
NJDOT forces took a total of ten (10) pavement cores and the thickness of UTW and AC for each core was recorded. Of the extracted cores only 3 were debonded at the interface. Other cores showed a strong bond at the interface but were broken in AC layer presumably due to coring operation.

The average UTW thickness was 3.8 inches with the thinnest being 2.9 inches at core location 4.11 (in 4' by 4' section) and thickest being 4.6 inches at core location 3.1 (in 3' by 3' section). Average thickness of 3' by 3' slabs are 4.12 inches where for 4' by 4' and 6' by 6' are 3.2 inches and 3.65 inches, respectively.

The detailed thickness information is presented in Table 3 below:

Table 2.3: Core Results

Core Number	UTW Thickness (in)	AC Thickness (in)	Total Pavement (in)
3.1	4.6	6.5	11.1
3.12	4.2	5.2	9.3
3.13	3.8	7.0	10.8
3.15	4.0	7.3	11.3
3.9	4.0	6.4	10.4
4.11	2.9	7.4	10.2
4.14	3.4	6.3	9.7
4.16	3.3	6.9	10.2
6.12 (A)	3.7	6.7	10.4
6.12 (B)	3.6	6.5	10.1
Average	3.8	6.6	10.4



AREA	2,320 sq	U.T.C.	193 cy
<u>SAWCUTTING</u>		10,558.00 lf	

Figure 1.2: Schematics of Route I-295 Ramp UTW Overlay
Prepared by NJDOT

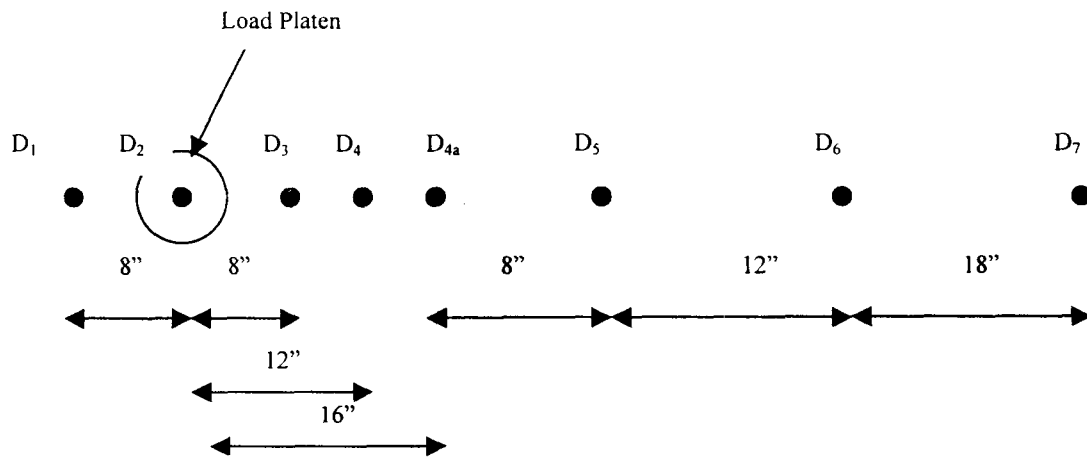


Figure 1.3: Geophone reconfiguration of Heavy (Falling) Weight Deflectometer for UTW Testing

CHAPTER 3

Finite Element Analysis and Verification

A finite element model was developed for the analysis of an AC pavement with UTW. The modeling and analysis was done by SAP2000 (Computers and Structures, Inc., 1997) structural analysis (finite element) program. The following sections contain the description of geometrical and material properties of the finite element model, loading conditions, and results of a parametric study conducted.

Finite Element Model Description

The finite element model of an AC pavement with UTW is shown in Fig. 3.1. In general the model describes a four-layer pavement, consisting of the UTW, AC base, granular subbase, and the subgrade. Seven layers of solid elements in the vertical direction describe this four-layer pavement. The top two layers represent the UTW layer. The third layer is used in the description of the AC-UTW interface. The following two layers indicate the AC layer. Finally, the bottom two layers represent the subbase. In addition to the solid element layers, the subgrade is described by a set of springs.

In the plan view, each of the UTW slabs, and the layers below, are discretized into 36 (6x6) elements, except the central (loading application) slab that is discretized into 144 (12x12) elements. An automated finite element model generator was developed for pavements with 3'x3' and 4'x4' UTW slab sizes. In the case of a 3'x3' UTW slab model the horizontal dimensions of solid elements are 3"x3" in the central area and 6"x6" elsewhere. In the case of a 4'x4' UTW slab the solid element dimensions are 4"x4" and 8"x8" inside and outside the central area, respectively.

Materials of all layers in the model are described as linearly elastic and isotropic, except the AC-UTW interface and UTW slab joints that are described as anisotropic materials.

The latter two are described as anisotropic to allow reduced load transfer from the UTW to AC layer due to layer debonding, and from one UTW slab to another due to joint cracking. A detail of an UTW slab joint is shown in Fig. 3.2.

Four loading conditions were investigated. The first loading case is a temperature gradient in the UTW layer. The temperature gradient is described by a linearly distributed temperature increase between the surface and the bottom of the UTW layer. The second loading case is a single axle load (SAL) of 18,000 lbs. applied at a corner of a UTW slab. The third and fourth loading cases are the loading at a joint and at the middle of the slab, respectively. The loaded area in the case of a 3'x3' UTW slab consists of two 6"x9" areas, spaced 12" one from the other. Each loading area is equivalent to a single tire loading of 4,500 lbs. In the case of a 4'x4' UTW slab, due to the 4"x4" element discretization, the approximation of the prescribed loading pattern is given by two 8"x8" loaded areas, spaced also 12" one from the other.

Prior to the development of the final finite element model, the effect of the size of the model was studied with objective to obtain the minimum size practically needed to accurately describe the behavior of a much wider pavement. The study was conducted on models having from 3 to 5 UTW slabs in both horizontal directions (Fig. 3.3). From the comparison of the stress and displacement results for the four loading cases, it was concluded that 4x4 (Fig. 3.1) and 5x5 produce values that do not differ more than 5%. This is illustrated in Fig. 3.4 for deflections, and maximum compressive and tensile flexural and vertical stresses in the UTW slab. Therefore, to achieve significant computational benefits, a 4x4 model was selected for further analyzes. The 4x4 model has about 9,500 joints with about 25,000 degrees of freedom, approximately 5700 solid elements, and about 900 spring elements.

Parametric Study

An extensive parametric study was conducted, with an objective to identify parameters that significantly affect the response of an AC pavement with an UTW overlay. The following parameters and their ranges were investigated:

- UTW thickness – 3 to 5 inches
- AC thickness – 4 to 8 inches
- AC modulus of elasticity – 880 to 1,660 ksi
- Subbase modulus of elasticity – 4.2 to 16.8 ksi
- Modulus of subgrade reaction – 145 to 580 pci
- UTW slab size – 3'x3' and 4'x4'
- Interface bonding – from fully bonded to unbonded, and
- Joint cracking.

The combined effect of the UTW and AC thickness and elastic modulus variation can be conveniently described by the corresponding flexural rigidities of their slabs. In all cases the following material properties were kept constant:

- Elastic modulus of UTW – 3,400 ksi
- Poisson's coefficient of UTW – 0.15
- Coefficient of thermal expansion of UTW – $0.38 \cdot 10^{-5} 1/^{\circ}\text{F}$
- Poisson's coefficient of AC – 0.35
- Thickness of the subbase – 1 ft
- Poisson's coefficient of the subbase – 0.35
- UTW-AC interface thickness – 0.5 inch
- Joint width – 0.5 inch, and
- Joint depth – 1/3 of the UTW slab thickness.

The UTW and AC layer thickness, AC thickness, AC stiffness, and UTW-AC bonding are the parameters that affect stresses in both UTW and AC the most. Figures 3.5 to 3.8 illustrate the effect of the thickness of UTW and AC layers on maximum tensile and compressive stresses in the same layers. The results are for a single axle loading and full bonding between UTW and AC. A satisfactory trend can be observed for both maximum tensile and compressive stresses. As the thickness of any of the layers increases, the maximum stress decreases. For the range of thicknesses and all the single axle loading conditions used in the analysis, the maximum tensile stress in UTW varies from about 29 psi for 5" UTW and 8" AC to about 45 psi for 3" UTW and 4" AC. Similarly, the maximum compressive stress in UTW varies from about 128 to 242 psi. The maximum tensile stress in the AC layer varies from about 50 to 148 psi. Both thicknesses have little effect on the maximum stresses in the UTW due to the temperature load. For the 10⁰F temperature difference the maximum tensile stress varies between about 23 and 26 psi, while the maximum compressive stress varies between about 81 and 88 psi.

Significantly stronger effect of the UTW and AC layer thickness on the maximum stress variation and much higher stress values are obtained for fully unbonded conditions. This is illustrated in Figs. 3.9 and 3.10 for maximum tensile stresses due to joint single axle loading in UTW and AC layers, respectively. The maximum tensile stress in UTW for all single axle loading positions varies from about 150 to 395 psi. A similar, but much more pronounced trend to that for the bonded case can be observed. The maximum compressive stress in the UTW varies from about 177 to 445 psi. The maximum tensile stresses in the AC layer due to the single axle loading vary between 76 and 184 psi. For the +10⁰F temperature difference there are no tensile stress in the UTW, while the maximum compressive stress in the UTW varies between about 113 and 148 psi. The maximum tensile stress in the AC due to the temperature gradient varies between about 3 and 13 psi, while the maximum compressive stress varies between about 7 and 12 psi. Typical maximum stress distributions for a joint single axle loading are shown in Figs. 3.11 and 3.12.

AC modulus affects the magnitude of the maximum stresses in a way similar to the AC layer thickness. This is due to a fact that the real effect is coming from the flexural rigidity of the AC layer, that is linearly proportional to the modulus and cubically proportional to the thickness. Figure 3.13 illustrates the effect of variation of the AC modulus on maximum compressive and tensile stresses in UTW and AC.

Other parameters such as joint cracking, subbase modulus, modulus of subgrade reaction, and the slab size, had minor effect on maximum stresses in both the UTW and AC. This is illustrated in Fig. 3.14 for the effect of variation of the AC modulus and modulus of the subgrade reaction on maximum compressive and tensile stresses in UTW and AC. Generally, an increase in the modulus of subgrade reaction reduces the maximum stresses. For the range of subgrade modulus studied, the stress variation is less than 10%. Higher joint cracking (reduced shear transfer) increases maximum stresses, while the increase from 3'x3' to 4'x4' UTW slabs had no effect on maximum stresses.

Finally, because the most cracking on the I-295 ramp was observed along the construction joints, possible effects of those on maximum stresses were studied. Two model modifications were considered. The first modification involved complete separation between UTW slabs along one joint line. The second modification involved, in addition to the first, a crack propagation through the AC below the joint line. The following observations can be made from the comparison of the obtained results. Presence of a construction joint does not increase the maximum tensile flexural stresses in the UTW due to wheel loading, in comparison to the joint-free case, however it increases by about 20% due to the temperature gradient. Also, it increases maximum stresses in the AC for all loading conditions by about 25%. As the crack in the AC layer is added, the maximum stresses in the UTW increase by about 25%, in comparison to the joint-free case, and 1-3% higher stresses in the AC layer. For an unbound system, the

maximum tensile stresses in UTW and AC increase by about 35% and 50%, respectively. The temperature stresses are also %35 higher for an unbound system with cracked AC.

From the above observation, it is concluded that a construction joint in UTW increases the tensile stress in AC. If the AC cracks as well, the stress in AC is relaxed, but the stress in UTW is increased. This problem requires further study to make more comprehensive conclusions about the effects of construction joints on the performance of AC pavements with an UTW overlay.

Finite Element Model Verification

To verify the finite element model, a simple case that the theoretical results from the Westergaard equation are available is considered. Westergaard (1927) developed closed form equations for maximum stresses in a slab resting on an elastic foundation due to several load conditions. For a load at the center of a slab where the effect of joints can be neglected, the maximum flexural stress in the slab can be approximately expressed as:

$$\sigma = \frac{0.316P}{h^2} \left[4 \log\left(\frac{l}{b}\right) + 1.069 \right] \quad 3.1$$

Where P is the applied load, h is the slab thickness; b indicates the size of the resisting section of the slab; that is

$$\begin{aligned} b &= \sqrt{1.6r^2 + h^2} - 0.675h & \text{if } r < 1.724h \\ b &= r & \text{if } r \geq 1.724h \end{aligned} \quad 3.2$$

in which r is the radius of the applied load. Finally, l is the radius of relative stiffness

$$l = \sqrt[4]{\frac{Eh^3}{12(1-\mu^2)k}} \quad 3.3$$

where E and μ indicate the elastic modulus and Poisson's ratio of the slab respectively, and k represents the coefficient of subgrade reaction.

The maximum tensile stress in a 3-inch thick concrete slab with an elastic moduli of 3400 ksi and Poisson's ratio of 0.15, resting on an elastic foundation with a coefficient of subgrade reaction of 250 pci, under a 12000-pound tire load that has 50 psi air pressure is calculated as 758 psi. The maximum tensile stress from the finite element model is obtained as 785 psi. The relative error is %3.5 which is basically due to the conversion of the circular tire load in Westergaard equation to joint loads in the finite element model.

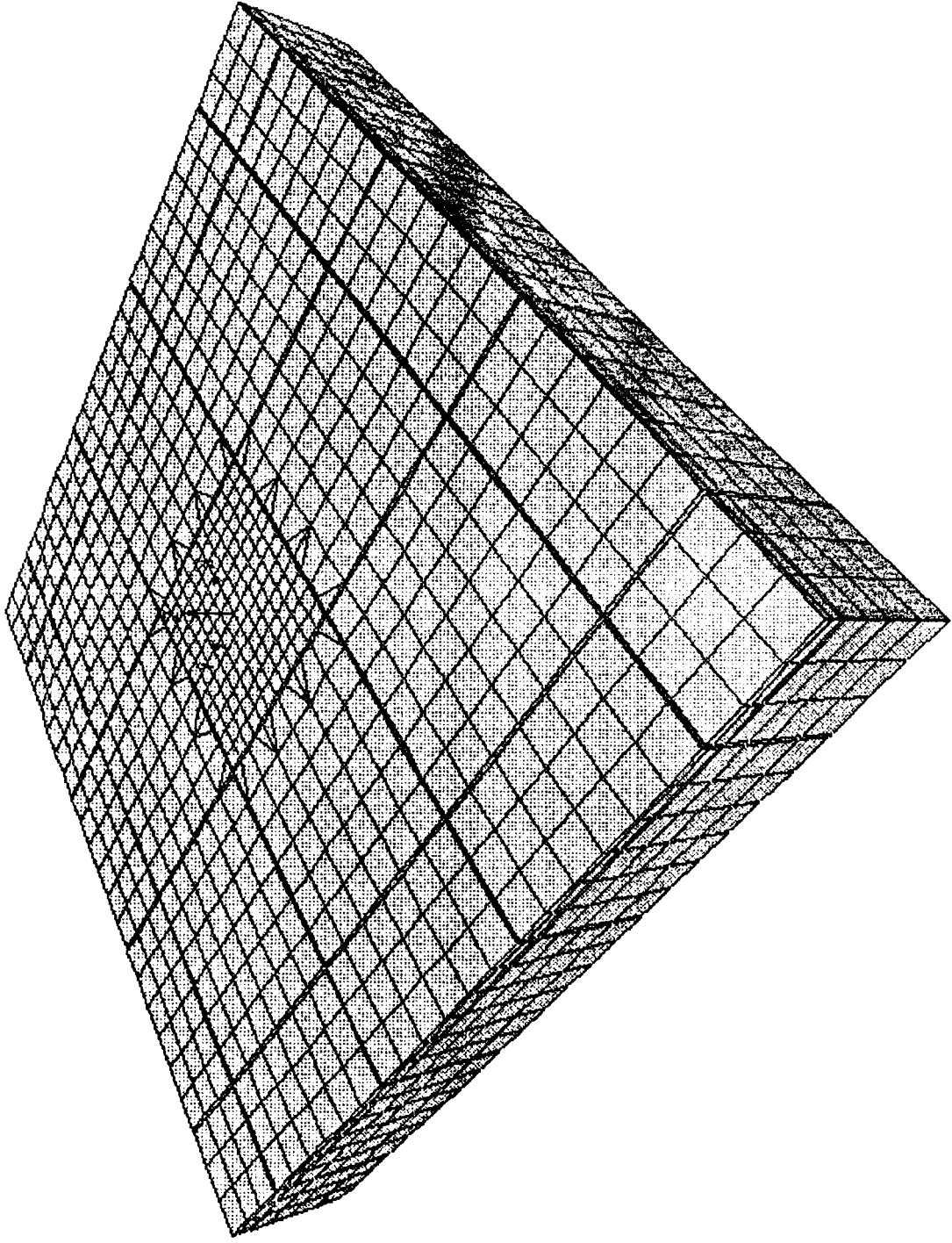


Figure 3.1. Finite element model.

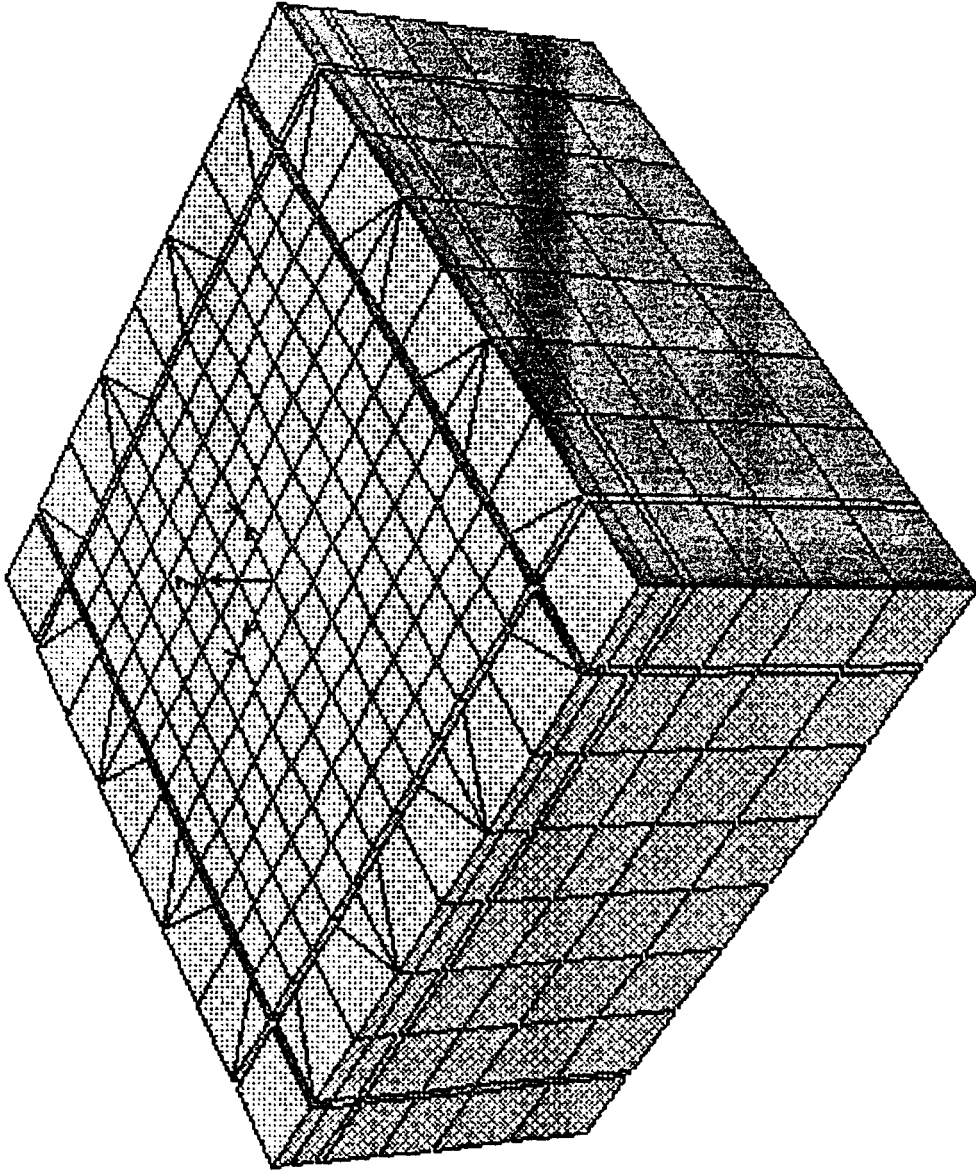


Figure 3.2. Detail of the finite element model.

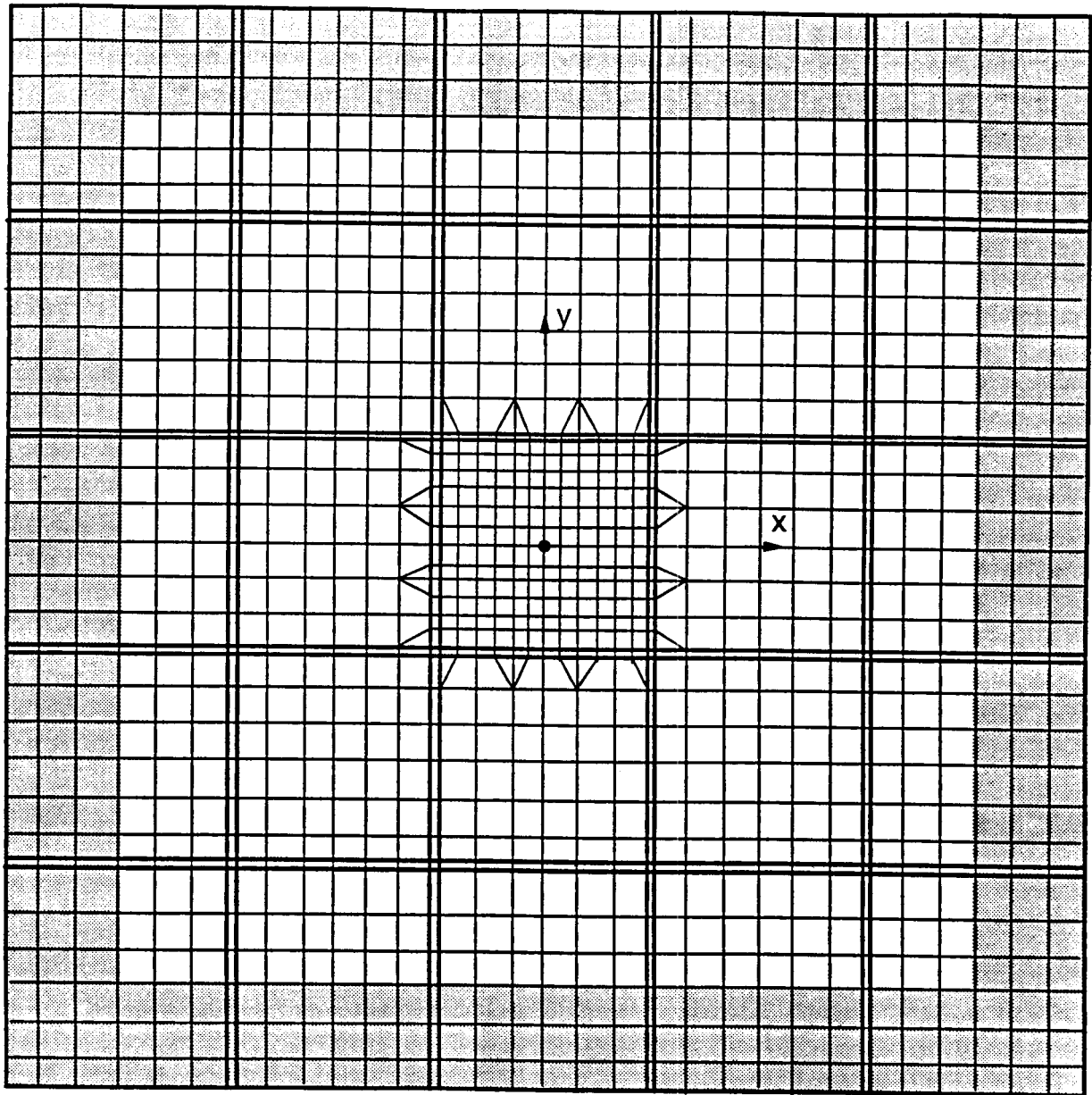
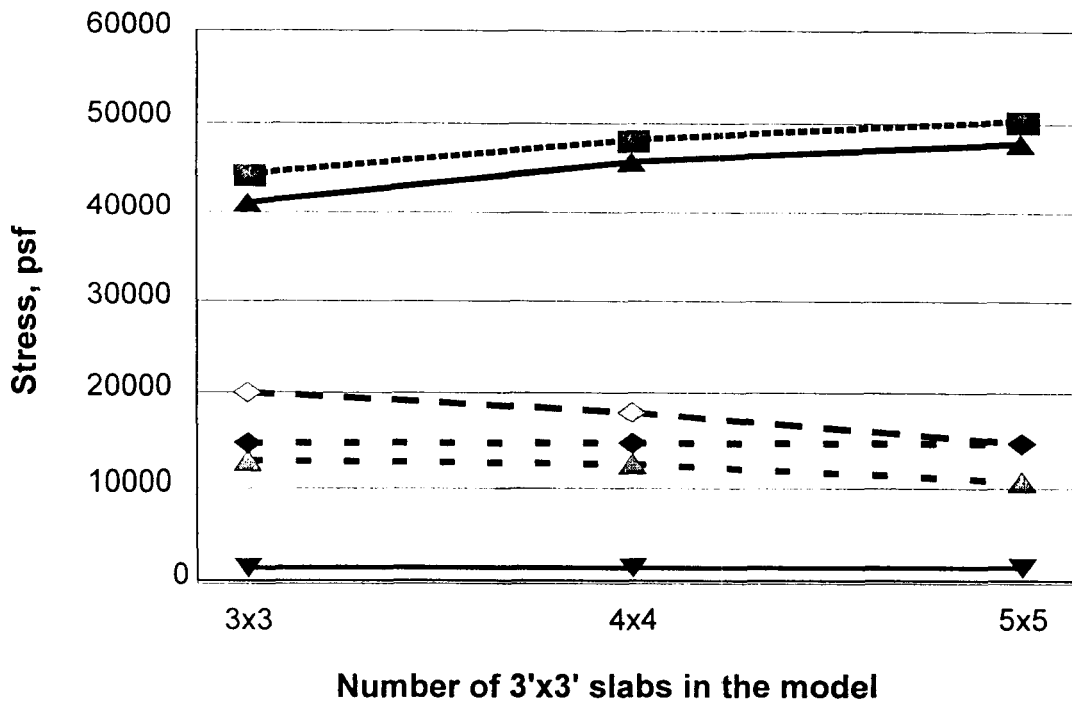
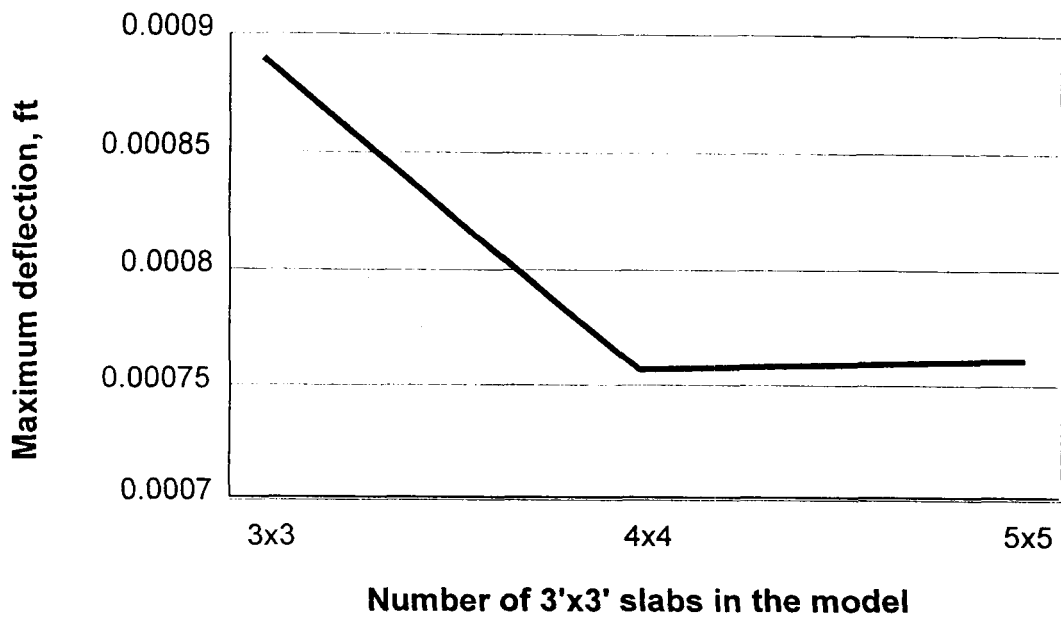


Figure 3.3. Plan view of models analyzed in the model size study.



$\sigma_{xx\ c}$ $\sigma_{xx\ t}$ $\sigma_{yy\ c}$ $\sigma_{yy\ t}$ $\sigma_{zz\ c}$ $\sigma_{zz\ t}$
 - - - ■ - - - - ◇ - - - - ▲ - - - - ▼ - - - - ◆ - -

Figure 3.4. Maximum deflections and compressive and tensile stresses in UTW as a function of size of the model.

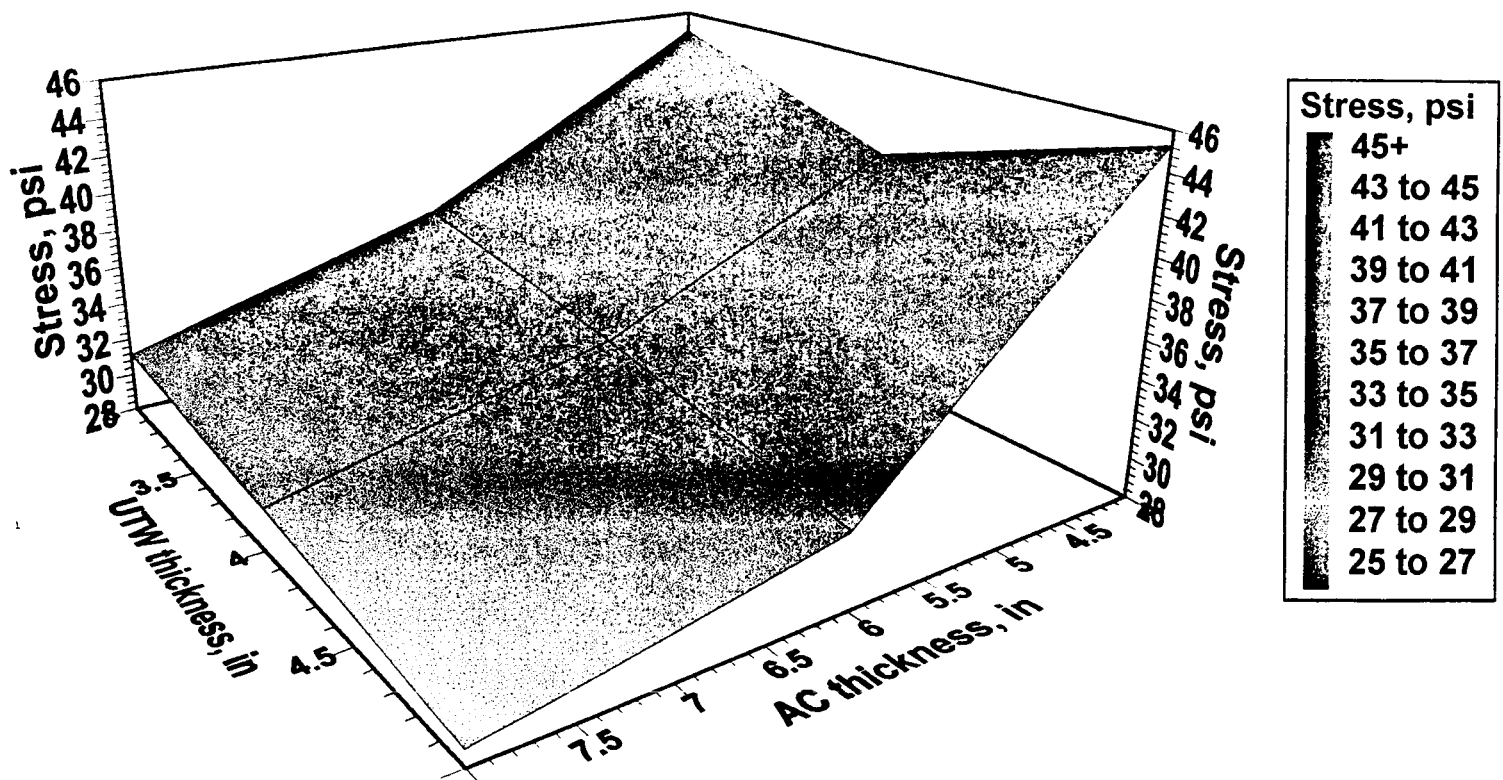


Figure 3.5. Maximum tensile stresses in UTW as a function of UTW and AC thicknesses. Corner load. Fully bonded.

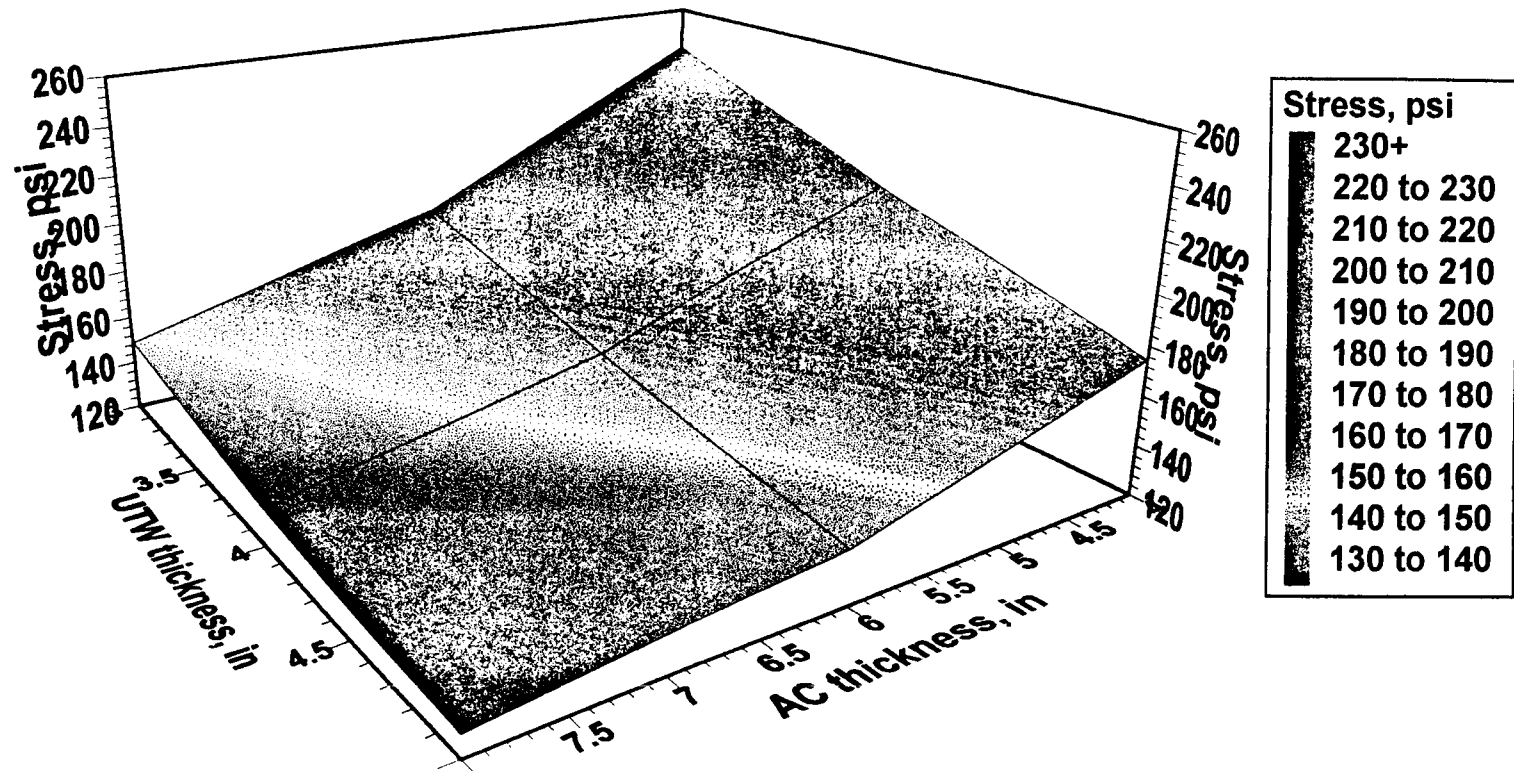


Figure 3.6. Maximum compressive stresses in UTW as a function of UTW and AC thicknesses. Corner load. Fully bonded.

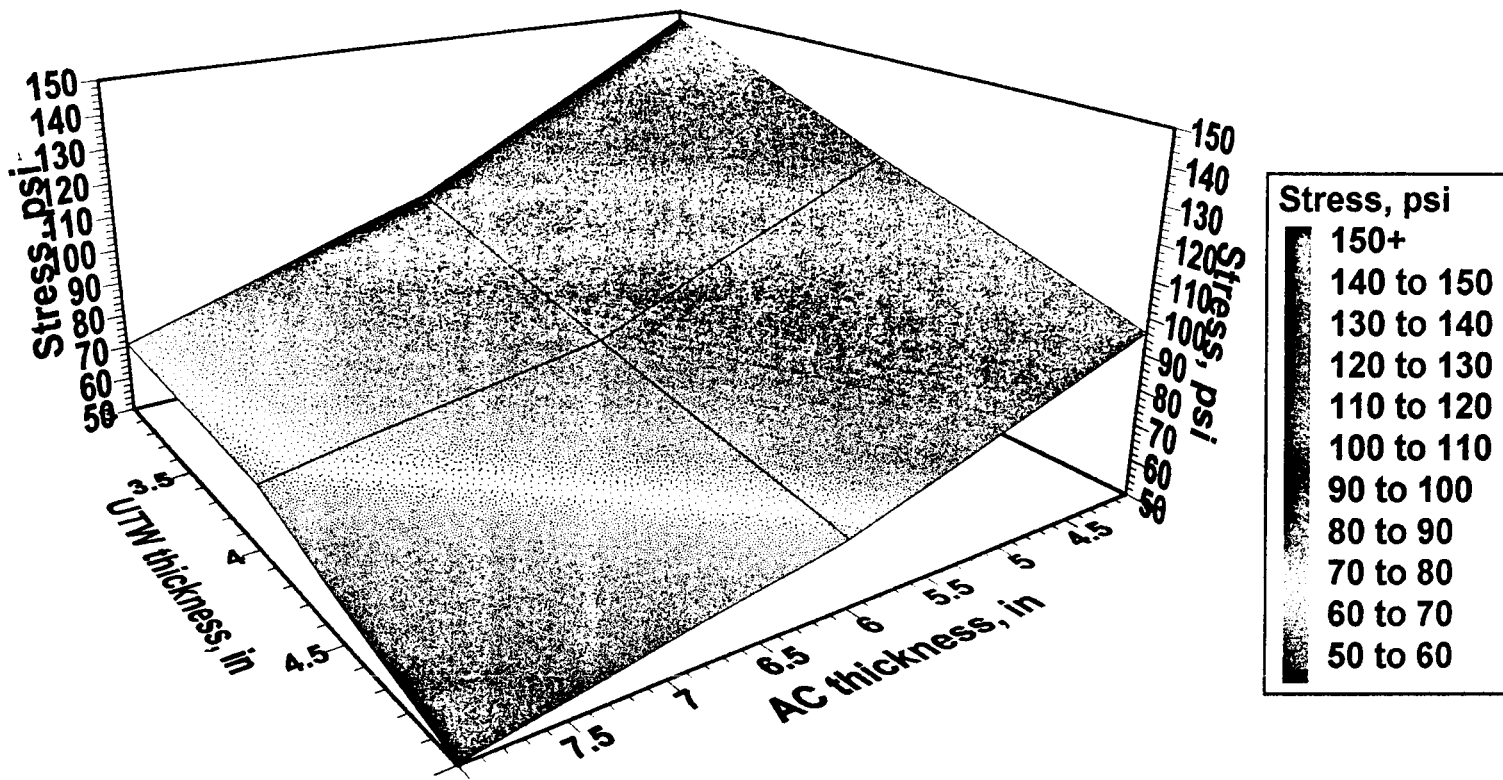


Figure 3.7. Maximum tensile stresses in AC as a function of UTW and AC thicknesses. Corner load. Fully bonded.

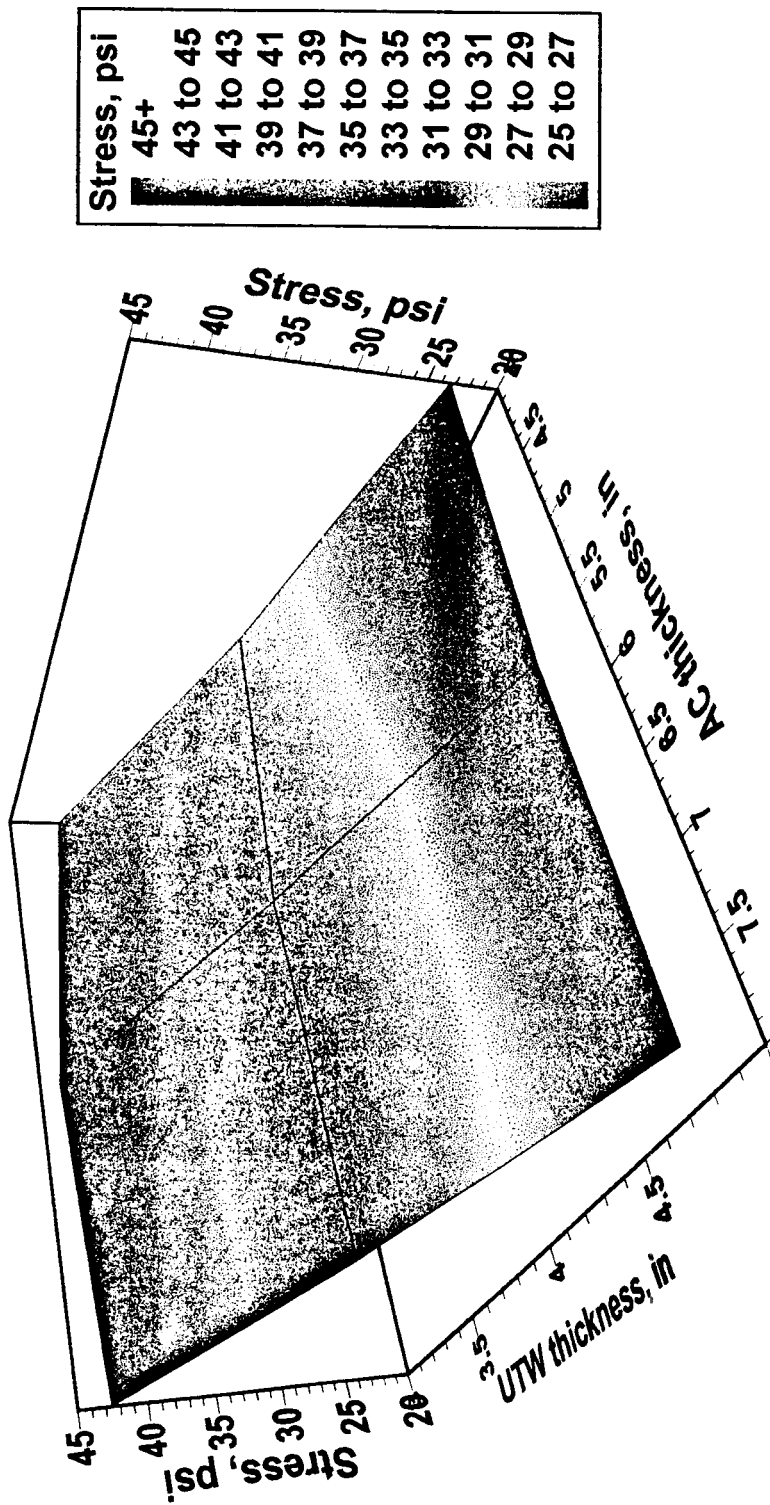


Figure 3.8. Maximum compressive stresses in AC as a function of UTW and AC thicknesses. Corner load. Fully bonded.

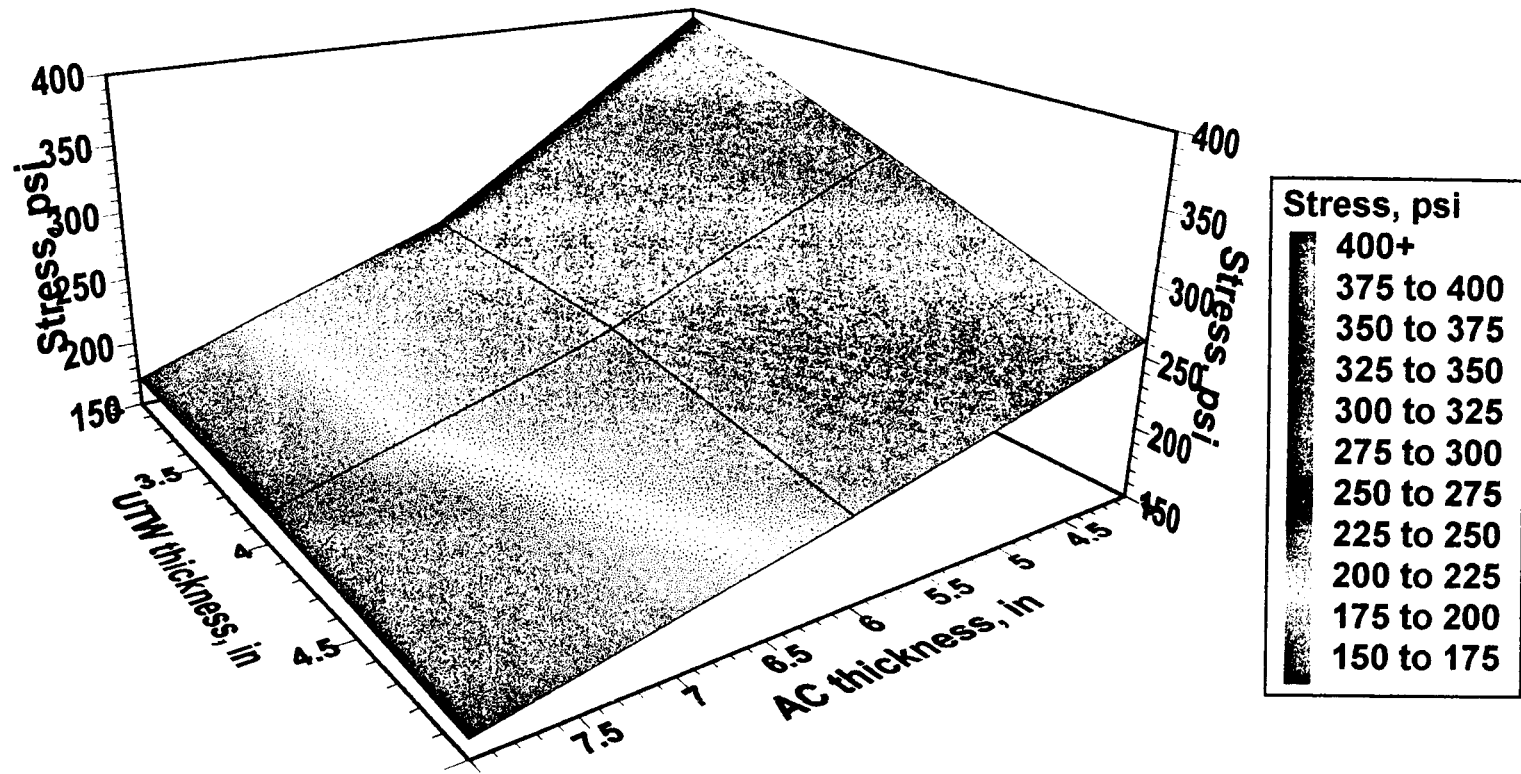


Figure 3.9. Maximum tensile stresses in UTW as a function of UTW and AC thicknesses. Single axle load. Unbonded.

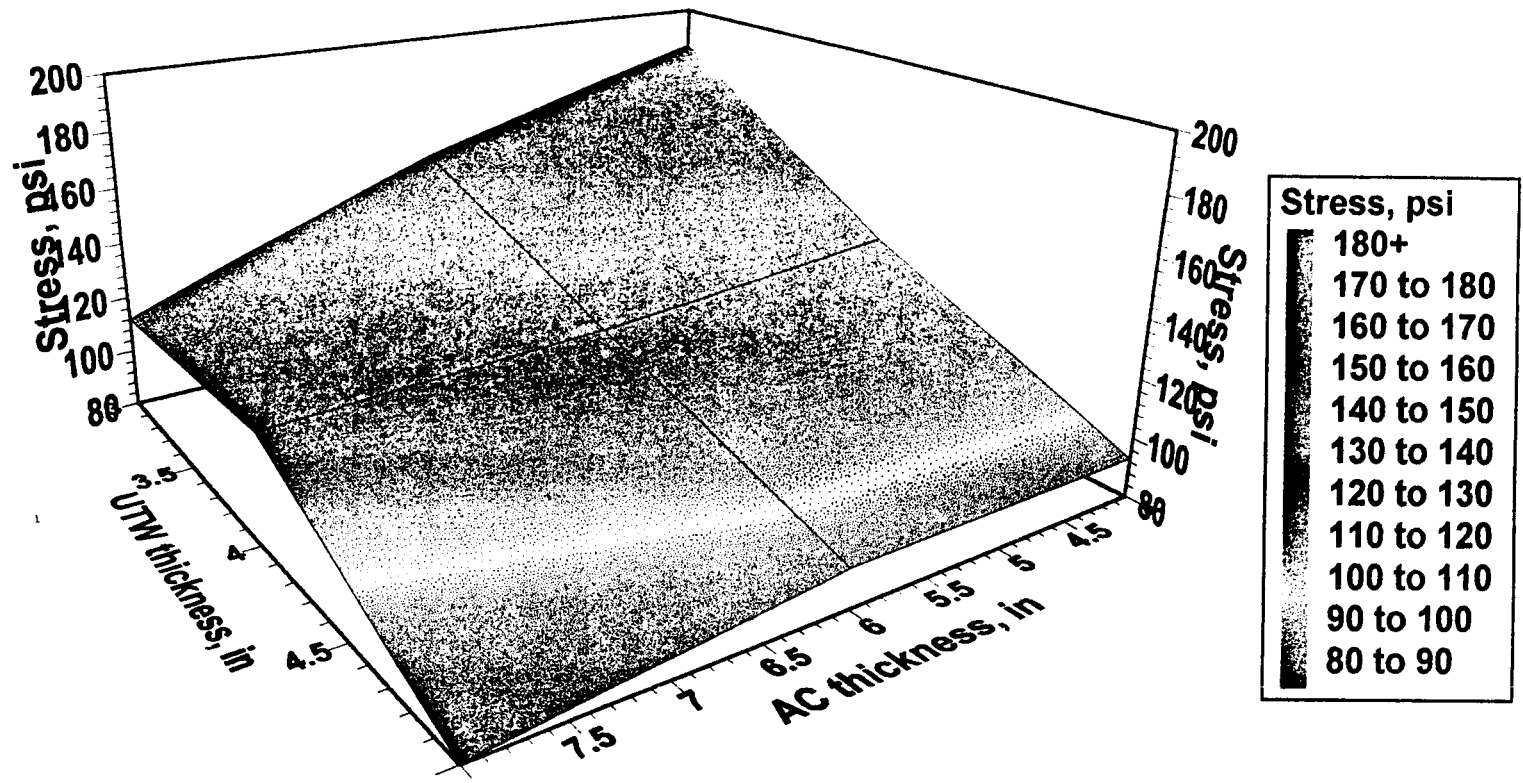


Figure 3.10. Maximum tensile stresses in AC as a function of UTW and AC thicknesses. Single axle load. Unbonded.

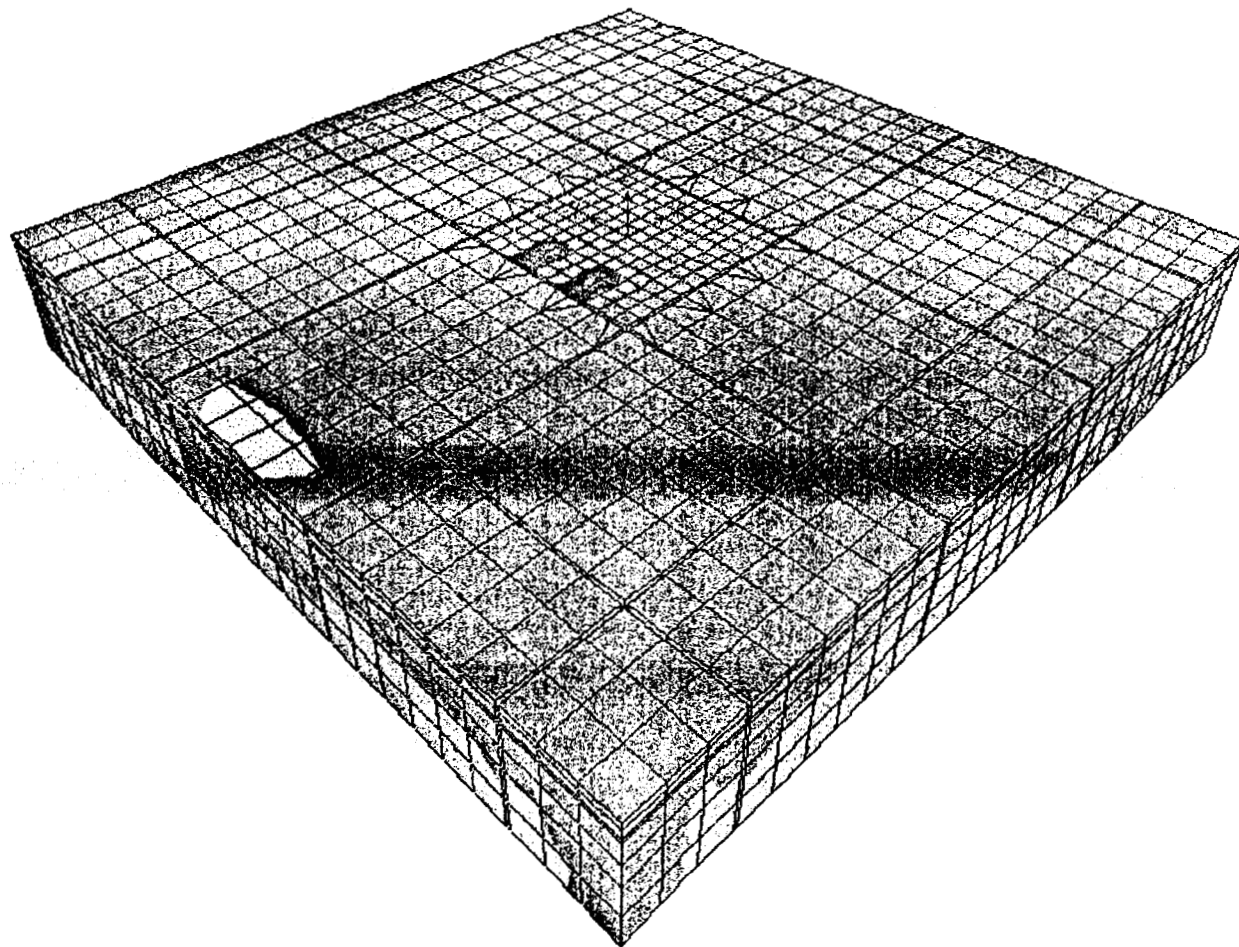
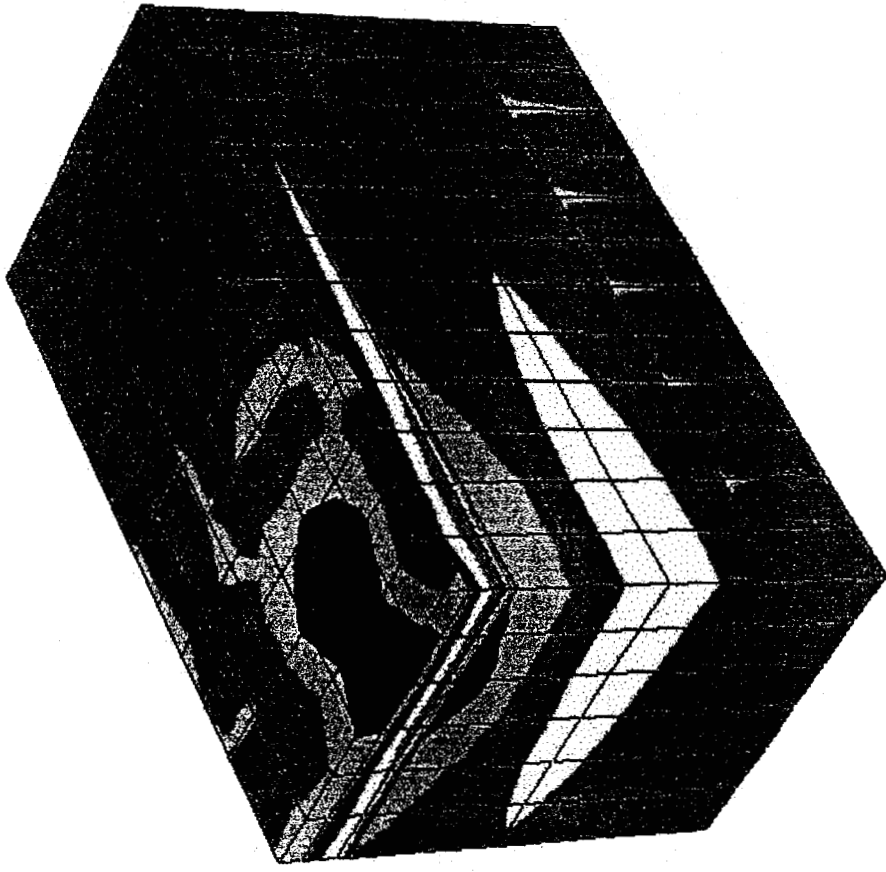


Figure 3.11. First principal stress distribution (psf). 3" UTW, 8" AC. Joint loading. Unbonded.





0 8 16 20.0 E+3

Figure 3.12. First principal stress distribution (psf). 3" UTW, 8" AC. Joint loading. Unbonded.

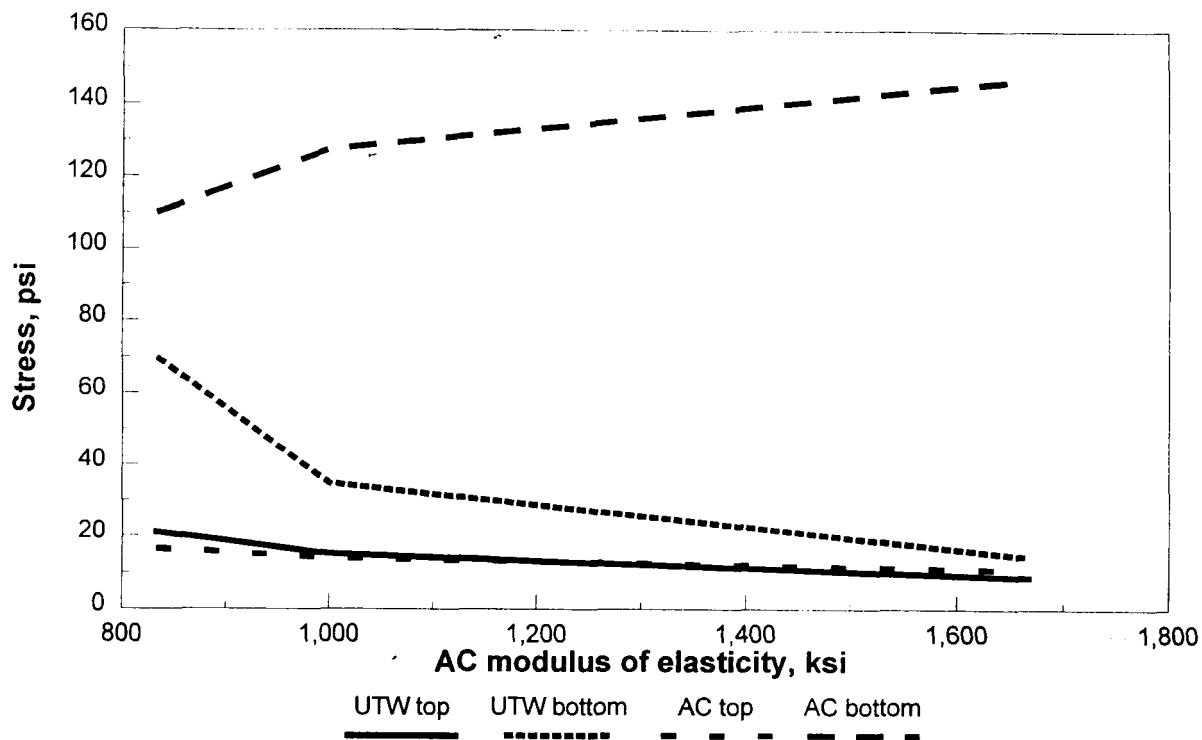


Figure 3.13. Effect of AC modulus of elasticity on maximum compressive flexural stresses in x direction. Corner loading, bonded.

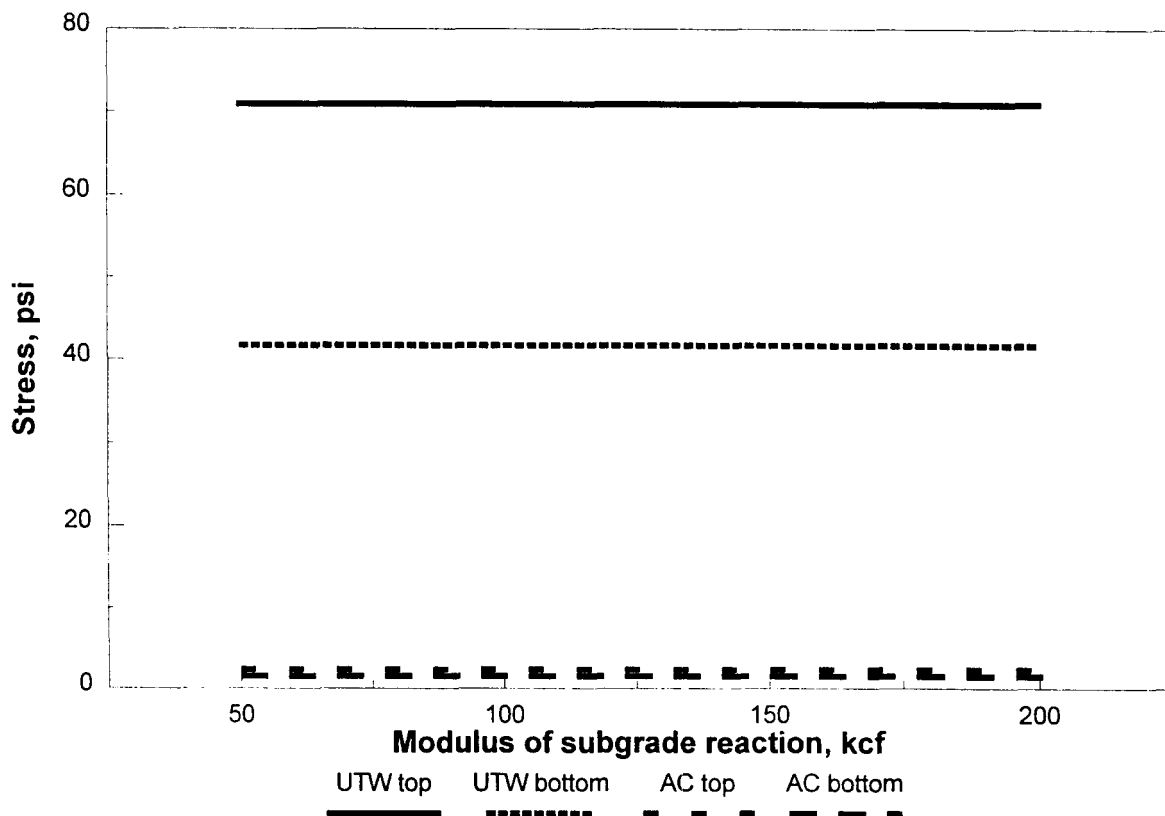


Figure 3.14. Effect of modulus of subgrade reaction on maximum tensile flexural stresses in x direction. Corner loading, bonded.

CHAPTER 4

Design Procedure

Essential parameters for a design procedure are stress levels in the pavement system, fatigue criterion of the materials used, traffic data, and environmental conditions. The design procedure in this study is based on the stress analysis in the pavement system under a dual tire single axle load.

Stress Due To Load

Since a finite element study can be very time consuming when used as a design tool, a series of equations is developed to predict the design stresses in a UTW pavement system based on the finite element results of this study.

It was mentioned in the previous chapter that the maximum stresses induced in a concrete slab on an elastic subgrade under a single load from the finite element model matches the Westergaard equation closely. A UTW system, however, is different from a slab on elastic foundation due to the existence of the AC layer and the saw cut joints. The composite beam concept is used to convert the concrete section to an equivalent asphalt section (Fig 4.1).

$$N.A. = \frac{nc^2 + a^2 + 2ac}{2(nc + a)} \quad 4.1$$

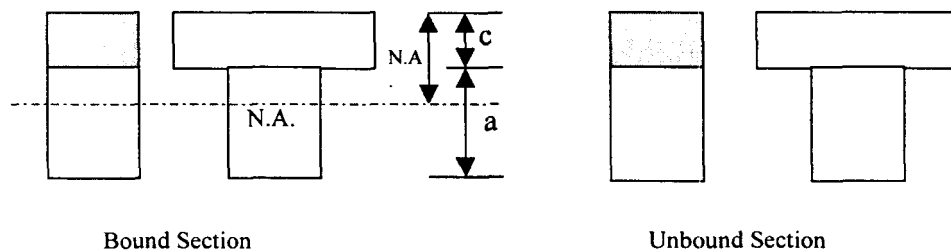


Fig. 4.1. Composite beam concept for bound and unbound cases.

where $N.A.$ is the depth of the Neutral axis from the top surface (UTW surface) in inches, c and a are the thickness of concrete (UTW) and asphalt in inches, respectively, and n is the ratio of elastic modulus of concrete to that of the asphalt.

$$n = \frac{E_c}{E_a} \quad 4.2$$

The section moment of inertia was determined for both bound and unbound conditions.

$$I_B = \frac{nc^3}{12} + \frac{a^3}{12} + \frac{nca(a+c)^2}{4(nc+a)} \quad 4.3$$

and

$$I_U = \frac{nc^3}{12} + \frac{a^3}{12} \quad 4.4$$

The size of the resisting section of the slab l and the radius of relative stiffness b are obtained from Eq. 3.2 and 3.3, respectively, with $h^3/12$ being replaced by the section moment of inertia. The prediction equation for maximum tensile stress in AC for a bound case is developed as

$$\sigma_B^{AC} = \frac{CP(N.A.-h)}{I_B} \left[C_1 \log\left(\frac{l}{b}\right) + C_2 \frac{N.A.}{a} + C_3 \right] \quad 4.5a$$

where C_1 , C_2 , and C_3 are constants obtained from a least square analysis based on the finite element results as listed in Table 4.1. The C factor indicates the contribution of the other wheel of the single axle (about 1.1) or the influence of a construction joint.

Similarly, the maximum tensile stresses in UTW for a bound case, in AC for unbound case, and in UTW for unbound case are

$$\sigma_B^{UTW} = \frac{CPn(N.A.-c)}{I_B} \left[C_1 \log\left(\frac{l}{b}\right) + C_2 \frac{N.A.}{c} + C_3 \right] \quad 4.5b$$

$$\sigma_U^{AC} = \frac{CPa}{2I_U} \left[C_1 \log\left(\frac{l}{b}\right) + C_2 \frac{a}{h} + C_3 \right] \quad 4.5c$$

$$\sigma_U^{UTW} = \frac{CnPc}{2I_U} \left[C_1 \log\left(\frac{l}{b}\right) + C_2 \frac{c}{h} + C_3 \right] \quad 4.5d$$

The average error of predicted stress values from Eqs. 4.5a to 4.5d are 2.3, 57.5, 2.6, and 2.9%, respectively. The large average error value for Eq. 4.6 is due to the small values of tensile stress in UTW for most of the cases considered in finite element study. However, because the small tensile stresses are not of concern for design purposes, the equation can be satisfactory used. The average error for tensile stresses of larger than 150 psi is 4.7%.

In Appendix G, the stress values from prediction equation are verified.

Table 4.1. Values of constants C, C₁, C₂, and C₃ in Eqs. 4.5a to 4.5d.

	Maximum tensile stress in	C		C ₁	C ₂	C ₃
		Construction Joint	No Construction Joint			
Bound	Asphalt Concrete	1.25	1.1	-0.2018	-0.0075	-0.0414
	Portland Cement Concrete	1.25	1.1	-0.2815	0.3479	-0.2384
Unbound	Asphalt Concrete	1.50	1.1	0.3460	-0.1767	0.1069
	Portland Cement Concrete	1.35	1.1	0.3152	-0.0960	0.0350

Stress Due To Temperature

Temperature variation over the thickness of concrete slabs causes warping of the slab and introduces flexural stresses. The magnitude of the warping stress depends on the temperature difference between the top and bottom of the slab, the elastic modulus and the coefficient of thermal expansion of the slab, as well as the slab rigidity. Based on the finite element results, the following prediction equation for the maximum temperature induced tensile stress in the slab is developed

$$\sigma_T = CE_c\alpha\Delta T \left[C_4 \frac{c}{l} + C_5 \right] \quad 4.6$$

in which E_c and α are the concrete elastic modulus and coefficient of thermal expansion respectively, and ΔT is the temperature difference between the top and bottom of the slab. The constant C implements the effect of a construction joint, and constants C_4 and C_5 are obtained from least square analysis. Table 4.2 shows the values of C , C_4 , and C_5 for bound and unbound cases.

The temperature variation does not introduce significant stresses in AC layer.

Table 4.2. Values of coefficients C , C_4 and C_5 in Eq. 4.6

	C		C_4	C_5
	Construction Joint	No Construction Joint		
Bound	1.20	1.0	-0.35	0.48
Unbound	1.35	1.0	0.35	0.48

Design Stresses

Construction Joint. The stress values obtained from Eq. 4.5 include the influence of the other wheel of a single axle through C factor. If there are construction joints the design stresses should be increased to consider the fact that the tire load is not transferred to the other side of the joint, while the contribution of the other wheel to the tensile stresses should be dropped. The C factor in the case of a construction joint, based on the finite element results mentioned in Chapter 3, is 25%, 25%, 50%, and 35% for Eq. 4.5a to 4.5d, respectively. The tensile stress due to temperature should also be increased by %20 if a construction joint exists. Table 4.3 summarizes the stress magnification factor for joints.

Table 4.3. Adjustment factor C for design stresses close to a construction joint.

Stress due to	Wheel load (AC)	Wheel load (UTW)	Temperature (UTW)
Bound	1.25	1.25	1.20
Unbound	1.50	1.35	1.35

Temperature Gradient. During the day, the UTW surface is warmer than its bottom causing compressional flexural stresses to develop at the bottom of the UTW layer. The flexural stresses can be calculated using Eq. 4.6. The compressional stress reduces the damage caused by the wheel load. During the night, the reverse situation happens and the load damage increases. A very conservative approach is to ignore the reduction of tensile stress during the day and add temperature-induced stress to the wheel load stress for the whole traffic. Another approach is to assume that the positive and negative effect of differential temperature during the day and night cancel each other, i.e. ignore the effect of differential temperature.

Fatigue Criterion

Fatigue equations, developed by the Asphalt Institute and Portland Cement Association, are used in the design procedure of this study. The asphalt fatigue criterion is

$$N = 0.058 \frac{E_a^{2.437}}{\sigma^{3.291}} \quad 4.7$$

where N is the number of load repetition before failure (%10 cracking), E_a indicates asphalt elastic modulus, and σ is the maximum tensile stress in asphalt. The fatigue criterion for UTW is

$$N = \begin{cases} 10^{12.1(0.972-SR)} & SR > 0.55 \\ \left(\frac{4.258}{SR - 0.4325} \right)^{3.268} & 0.55 > SR > 0.45 \\ \infty & SR < 0.45 \end{cases} \quad 4.8$$

where SR is the ratio of tensile stress to the rupture stress of the Portland cement

$$SR = \frac{\sigma}{S'_c} \quad 4.9$$

concrete. The rupture stress S'_c can be estimated from the concrete elastic modulus (AASHTO 1993)

$$S'_c = \frac{43.5E_c}{1000000} + 448.5 \quad 4.10$$

in which E_c and S'_c are in psi. It is a good practice to keep SR below 45% so that the UTW can handle unlimited number of ESAL's.

Traffic Data

The traffic data, which is a combination of different vehicles, is converted to an equivalent 18-kips single axle to be used in Eqs. 4.7 and 4.8. The conversion is based on the fact that the fatigue criterion is a nonlinear function of design stress. It is desirable to let the failure of the asphalt layer govern the design, because asphalt should not fail prior to the overlain UTW. Thus, the asphalt fatigue criterion is chosen as the basis for traffic conversion.

$$W_{18} = \left(\frac{W_{SAL}}{18} \right)^{3.3} \quad 4.11$$

In the above equation, W_{18} is the factor to convert a single axle weighing W_{SAL} to an equivalent 18-kips single axle load. Tandem axles weighing double a single axle cause more than twice the damage to the pavement than the single axle load, because the axles are close to each other and each axle contributes to the stress under the other axle. The Eq. 4.11 for tandem axles changes to

$$W_{18} = \left(\frac{TW_{TAL}}{2 \times 18} \right)^{3.3} \quad 4.12$$

in which W_{TAL} indicates the weight of a tandem axle (both axles together) and T is a factor that indicates how much stress an axle introduces underneath the other axle. The tandem factor depends on the configuration of tires and the radius of the relative stiffness of the pavement system. Based on the influence charts for stresses in concrete pavements (Pickett and Ray 1951) the tandem factor T is roughly 1.25.

It should be mentioned that the 18-kips equivalent factor used in AASHTO 1993 is approximately proportional to the fourth power of the ratio of axle load under question to

18 kips. The power in the design procedure here is 3.3. If detail traffic data is not available, one may choose to use the 18-kips equivalency factor based on AASHTO.

Safety Factor

It is recommended that the same concept found in AASHTO 1993, be used for safety factor (i.e. increase the number of design ESAL based on the standard deviation of errors in traffic prediction and pavement performance, and the required design reliability).

$$W_D = 10^{-Z_R S_0} W_{18} \quad 4.13$$

where S_0 is the overall standard deviation of errors in design and Z_R is the standard normal deviate associated with design reliability. AASHTO recommends a standard deviation S_0 of 0.30 to 0.40 for rigid pavements and 0.4 to 0.5 for flexible pavements. Table 4.4 shows the values of Z_R based on the require design reliability R .

Table 4.4. Design reliability factors.

$R=$	70	80	85	90	91	92	93	94	95	96	97	98	99	100
$Z_R=$	-0.5	-0.8	-1.0	-1.3	-1.3	-1.4	-1.5	-1.6	-1.6	-1.8	-1.9	-2.1	-2.3	-3.8

Design Procedure

The following UTW design procedure is recommended.

- 1- Obtain the traffic data for the project and find the number of equivalent 18-kips single axle load from Eqs. 4.11, 4.12, and 4.13.
- 2- Obtain the elastic modulus and thickness of the existing asphalt pavement, as well as the coefficient of subgrade reaction. In-situ testing such as Falling Weight Deflectometer may be used to obtain moduli. Subtract the depth of milling from the AC thickness.
- 3- Calculate the allowable tensile stress in AC from Eq. 4.7.
- 4- Assume a thickness for UTW and find the maximum tensile stress in AC from Eqs. 4.5a and 4.5b for both bond and unbound conditions.
- 5- Compare the maximum tensile stress in AC against the allowable stress from Step 3.
- 6- Repeat Steps 4 and 5 until the allowable stress and maximum tensile stress are equal.

- 7- Calculate the maximum tensile stress in UTW due to both axle load and temperature differentials from Eqs. 4.5b, 4.5d, and 4.6.
- 8- Obtain the stress ratio SR in UTW and determine the maximum allowable number of load repetitions from Eq. 4.8.
- 9- If the UTW fatigue criterion indicates a smaller number of ESAL's than W_D , increase the UTW thickness and repeat Steps 4 to 9.
- 10- Choose the final UTW thickness by comparing bound and unbound design process.

Design Example

As an example the following information is assumed available for a UTW design project:

Number of ESAL's from traffic data, $W_{18}=1,000,000$

AC elastic modulus $E_a=500$ ksi

AC thickness after milling, $a=6$ in

UTW elastic modulus $E_c=5000$ ksi

UTW coefficient of thermal expansion $\alpha=0.0000038$ /°F

Coefficient of subgrade reaction $k=250$ pci

Tire pressure=80 psi

Standard deviation, $S_\sigma=0.4$

Required design reliability, $R=0.80$

Temperature differential=3°F/in

Design

$$Z_R = -0.8$$

(Table 4.4)

$$W_D = 10^{0.8 \times 0.4} \times 1000000 = 2100000$$

Equation 4.13

$$\sigma = \sqrt[3.29]{\frac{0.058 \times 500000^{2.437}}{2100000}} = 84 \text{ psi}$$

Equation 4.7

$$r = \sqrt{\frac{9000}{3.14 \times 80}} = 6 \text{ in}$$

radius of tire contact area

Assume $c=3$ in, $h=3+6=9$ in

$$b = \sqrt{1.6 \times 6^2 + 9^2} - 0.675 \times 9 = 5.7 \text{ in}$$

Equation 3.2

$$N.A. = \frac{10 \times 3^2 + 6^2 + 2 \times 3 \times 6}{2(10 \times 3 + 6)} = 2.25 \text{ in}^3$$

Bound

Unbound

$$I_B = 142 \text{ in}^3$$

$$I_U = 41 \text{ in}^3$$

Equations 4.3 and 4.4

$$l = \sqrt[4]{\frac{500000 \times 142}{(1 - 0.15^2) \times 250}} = 23.2 \text{ in}$$

$$l = \sqrt[4]{\frac{500000 \times 41}{(1 - 0.15^2) \times 250}} = 17.0 \text{ in}$$

Equation 3.3

$$\sigma = \frac{1.1 \times 9000 \times (2.25 - 9)}{142} \left[-0.2018 \log\left(\frac{23.2}{5.7}\right) - 0.0075 \frac{2.25}{6} - 0.0414 \right] = 79 \text{ psi} \quad \text{Eq. 4.5a}$$

The maximum tensile stress in AC due to load is less than maximum tensile stress allowed by Eq. 4.7. Check for the stress in UTW.

$$\sigma = \frac{1.1 \times 9000 \times 10(2.25 - 3)}{142} \left[-0.2815 \log\left(\frac{23.2}{5.7}\right) + 0.3479 \frac{2.25}{3} - 0.2384 \right] = 78 \text{ psi} \quad \text{Eq. 4.5b}$$

$$\sigma_T = 1.0(5 \times 10^6)(3.8 \times 10^{-6})(3 \times 3) \left[-0.35 \frac{3}{23.2} + 0.48 \right] = 74 \text{ psi} \quad \text{Eq. 4.6}$$

Total tensile stress for UTW would be 78+74=152 psi. This value has to be checked against the rupture stress.

$$S'_c = \frac{43.5 \times 5000000}{1000000} + 448.5 = 666 \text{ psi} \quad \text{Equation 4.10}$$

$$SR = \frac{152}{666} = 0.23 \quad \Rightarrow \quad N = \infty$$

The chosen thickness for UTW is satisfactory for bound condition. Try unbound condition:

For AC the maximum tensile stress is

$$\sigma = \frac{1.1 \times 9000 \times 6}{2 \times 41} \left[0.3460 \log\left(\frac{17.0}{5.7}\right) - 0.1767 \frac{6}{9} + 0.1069 \right] = 111 \text{ psi} \quad \text{Eq. 4.5c}$$

For UTW the maximum tensile stress due to load and temperature are

$$\sigma = \frac{1.1 \times 10 \times 9000 \times 3}{2 \times 41} \left[0.3152 \log\left(\frac{17.0}{5.7}\right) - 0.0960 \frac{3}{9} + 0.0350 \right] = 553 \text{ psi} \quad \text{Eq. 4.5c}$$

$$\sigma_T = 1.0(5 \times 10^6)(3.8 \times 10^{-6})(3 \times 3) \left[0.35 \frac{3}{23.2} + 0.48 \right] = 90 \text{ psi} \quad \text{Eq. 4.6}$$

The total stress due to load and temperature would be 643 psi which leads to a high stress ratio. Thus, 3 in. of UTW is not satisfactory if no bounding between AC and UTW exists. However, this assumption is not realistic. One may use a linear interpolation between the bounded and unbounded condition. For example, for a 70% bounding, the stress in AC and UTW would be 89 and 299 psi, respectively. Therefore, a 3.5-in UTW is satisfactory.

I295 Ramp

As another example the I295 ramp is considered. From the results obtained by the Falling Weight Deflectometer (FWD), the elastic modulus of the asphalt for the first section of the ramp (3-foot panels) is approximately 280 ksi at 68°F. The backcalculated elastic modulus of the UTW is 4400 ksi. A 3°F-temperature variation per inch thickness of UTW and a coefficient of thermal expansion of 3.8×10^{-6} for UTW is assumed. Core results indicate the thickness of UTW and AC as 4 and 6.7 inches, respectively. A bound condition is considered for this ramp, because the core results indicate a good bounding (asphalt was milled before placing the UTW). Plugging these values into Eq. 4.5a, the maximum tensile stress in AC and UTW is calculated as

$$\sigma = \frac{1.1 \times 9000(2.52 - 10.7)}{282} \left[-0.2018 \log\left(\frac{23.85}{5.64}\right) - 0.0075 \frac{2.52}{6.7} - 0.0414 \right] = 49 \text{ psi}$$

$$\sigma = \frac{1.1 \times 9000 \times 15.7 \times (2.52 - 4)}{282} \left[-0.2815 \log\left(\frac{23.85}{5.64}\right) + 0.3479 \frac{2.52}{4} - 0.2384 \right] = 160 \text{ psi}$$

$$\sigma_T = 1.0(4.4 \times 10^6)(3.8 \times 10^{-6})(3 \times 4) \left[-0.35 \frac{4}{23.85} + 0.48 \right] = 85 \text{ psi}$$

The number of allowable 18-kips axles is obtained from the minimum of Eqs. 4.7 and 4.8

$$N = 3,000,000 \quad \text{bound}$$

According to NJDOT, the average daily traffic (ADT) for the ramp is 23800 with 10.8% of heavy trucks and an 18-kips equivalency factor of 1.536. Thus, the total number of ESAL's per day is $23800 \times 0.108 \times 1.536 = 3950$. The life of the pavement, therefore, is estimated as 760 days for bound condition.

At the center of the ramp a construction joint exists that developed cracks earlier than the ramp itself. According to Table 4.3, the construction joint increases the C factor from 1.1 to 1.25. This increases AC stress to 57 psi, which results in 1,900,000 allowable ESAL's. Thus, the life of the pavement adjacent to the construction joint is estimated as 480 days.

References

1. Cole, L.W., and Mohsen, J.P., "Ultra-Thin Concrete Overlays on Asphalt", Presented at the 1993 TAC Annual Conference, Ottawa, Ontario.
2. Brown, D., "Ultra-Thin Whitetopping Emerges as Rehab Technique," *Transportation Builder*, V7, No. 1, January 1995, pp37-41.
3. Risser, R.J., LaHue, S.P., Volgt, G.F., and Mack, J., "Ultra-Thin Concrete Overlays on Existing Asphalt Pavement," 5th International Conference on Concrete Pavement Design and Rehabilitation, Vol.2, April 1993, Purdue University, IN., pp. 247-254.
4. Tritsch, S., "Whitetopping, Technique Revives Burgeoning Kansas Thoroughfare," *Roads and Bridges*, September 1995, pp. 52-55.
5. Packard, R.G., "UTW Proves its Worth in Worldwide Tests," *Roads and Bridges*, July 1996, pp.15.
6. Armaghani, J.M., "Evaluation of Ultra-Thin Whitetopping in Florida," Presented at the 1997 TRB Conference, Washington D. C.
7. Draft "Development of Ultra-Thin Whitetopping Design Procedure," Construction Technology Laboratories, Inc., January 1997.
8. National Highway Institute, "Techniques For Pavement Rehabilitation," US Dept. of Transportation, FHWA, Sixth Edition, April 1997.
9. Pickett, G., Ray, G. K., "Influence Charts for Rigid Pavements," *Transactions, ASCE*, 1951.

APPENDIX A

THE HEAVY (FALLING) WEIGHT DEFLECTOMETER

The Heavy (Falling) Weight Deflectometer (HWD) (Figure A1), is an apparatus for in-situ, non-destructive testing of pavement structures. Traffic loading is emulated by applying load pulses in a controlled manner. Deflections of the pavement surface are recorded at increasing radial distances from the load. The deflection response is an indicator of structural capacity, material properties and pavement performance. Features of the HWD include the following:

- Up to 70 non-destructive tests can be completed per hour, each providing data comparable to that from trial pitting
- The load is representative of moving vehicles, resulting in appropriate pavement response
- Can be used throughout the year, provided the unbound layers are in a unfrozen condition
- Suitable for thick, stiff pavements due to accurate deflection measurement in microns

Type of Tests

- Deflection Basin Test to evaluate pavement material properties for Asphalt Concrete (AC) and Pavement Cement Concrete (PCC) pavements
- Joint/Crack Performance Test to measure joint/crack load transfer efficiency and detect voids

Deflection Sensor Spacing

AC Pavements

Deflection testing for AC pavements is performed on the outer wheel track. Seven deflection sensors are spaced at radial distances of typically 0, 12, 24, 36, 48, 60, and 72 inches (0, 305, 610, 914, 1219, 1524, and 1829 mm as illustrated in Figure A2).

PCC Pavements

For testing of PCC pavements, the test setup used is similar to that adopted by the Strategic Highway Research Program (SHRP) Long Term Pavement Performance (LTPP) program for evaluation of concrete pavements. Joint testing is conducted by placing the load platen with a diameter of 300 mm (11.81in) close to the slab corner with a deflection sensor on both sides of the joint (or crack). Seven sensors deflection are spaced at radial distances of typically -12, 0, 12, 24, 36, 60, and 72 inches (-305, 0, 305, 610, 914, 1,524, and 1,829 mm). Both "Approach Slab" and "Leave Slab" tests can be performed to evaluate the joint/crack performance (see Figure A3). Basin tests are also conducted to evaluate the integrity of the PCC slabs and to provide remedial design if necessary.

Other Pavements

Due to the fundamental approach used for analysis of HWD test data the device is

particularly suitable for investigating a wide range of pavement types at different construction stages. Typical pavements which can be tested include:

- Conventional AC or PCC pavements
- Concrete Block Pavements on bound or unbound foundations
- Composite AC/PCC pavements
- Pavement with stabilized base
- Recycled pavements
- Pavement foundations and subbase layers
- Rail road track beds
- Airfield and dock pavements

Loading

The magnitude of the applied load is recorded. This can be adjusted by changing the mass of the falling weights or the height from which they are dropped, in order to obtain a contact pressure on the pavement surface which approximates to the pressure exerted by the types of the vehicles using the pavement. For highway pavement testing, the load levels applied are in the range 6,000 to 16,000 lbs (26.7 to 71.2 kN). For airfield pavements, load levels up to 55,000 lbs (244.7 kN) can be applied.

Data Analysis

Using computer software, the deflection data is back-calculated to obtain the effective stiffness of each pavement layer including the subgrade. These in-situ effective stiffnesses are a fundamental measure of the engineering properties of the pavement materials. They are used either in isolation, or combined with other test data to:-

- ◆ Assess the condition of each pavement layer to identify where deterioration has occurred.
- ◆ Obtain a residual life of the pavement structure using both analytical and empirical techniques
- ◆ Design and recommend strengthening or remedial measures to achieve the required future design life.
- ◆ Obtain information on the spacing of the primary transverse shrinkage cracks in a cement stabilized bases
- ◆ Obtain information on load transfer and slab support adjacent to joints and cracks in PCC pavements
- ◆ Measure the condition of the equivalent foundation supporting PCC pavements, enabling an assessment of residual life

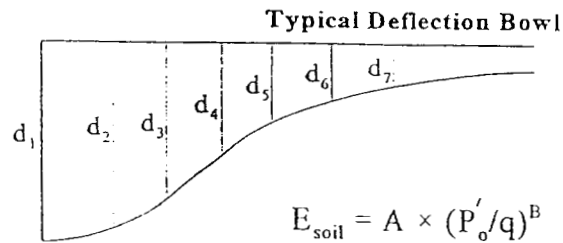
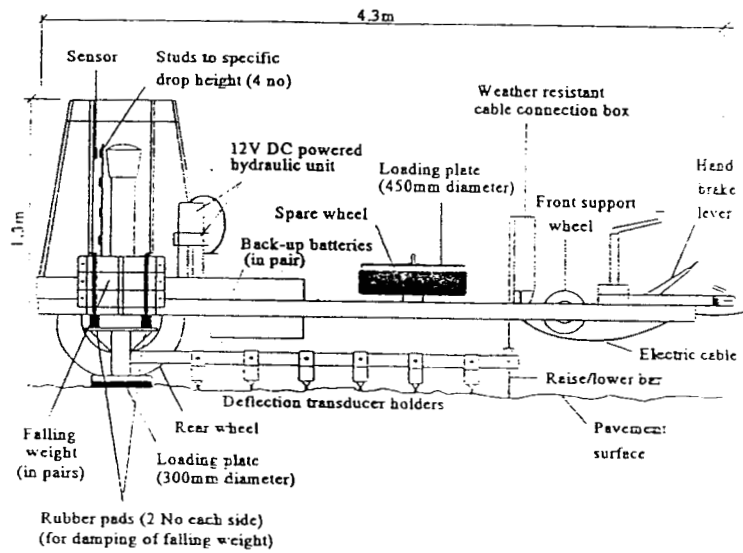
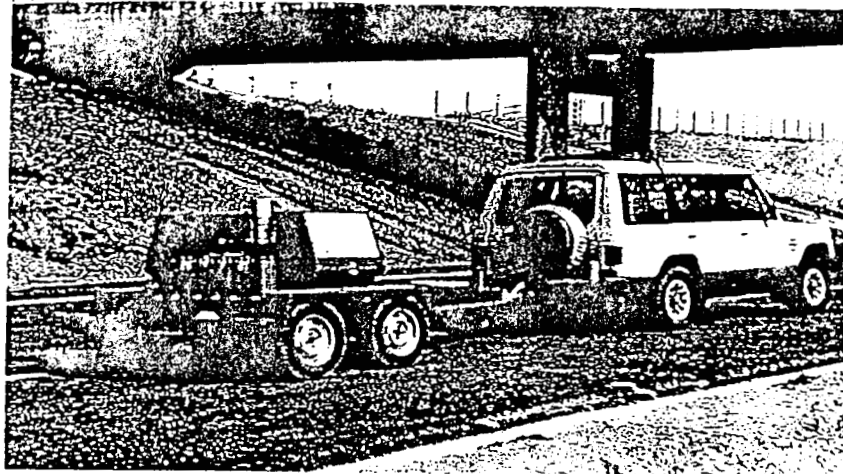


Figure A1: The Heavy (Falling) Weight Deflectometer

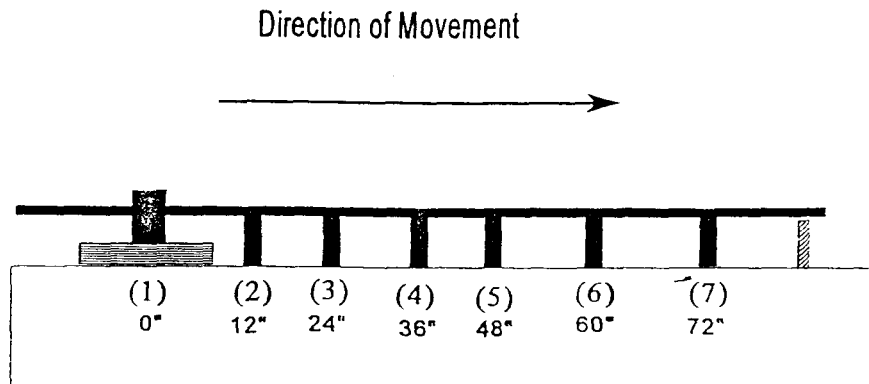


Figure A2: AC Pavement Testing

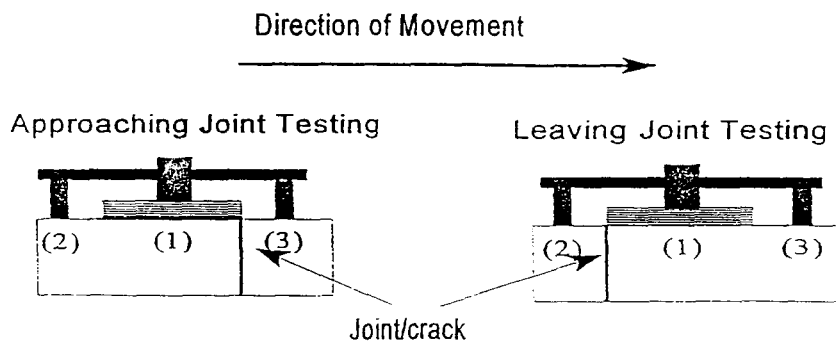
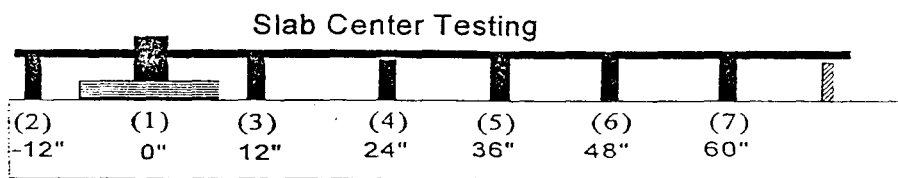


Figure A3: PCC Pavement Testing



New Jersey Concrete and Aggregate Association

1230 Parkway Avenue • Suite 101 • West Trenton • New Jersey 08628

(609) 771-00
FAX (609) 771-17

William J. Cleary, C.A.E.
Executive Director

NEW JERSEY DEPARTMENT OF TRANSPORTATION

ULTRA THIN CONCRETE OVERLAY

SPECIFICATIONS

DESCRIPTION:

This work shall consist of the placement of a special Portland Cement Concrete Surface Course, containing a number 8 size coarse aggregate, over an existing cleaned and milled flexible pavement.

MATERIALS:

Materials used in this construction shall meet the following requirements:

<u>Materials</u>	<u>Requirements</u>
Portland Cement	919.11
Water	919.15
Aggregates	901.13
Air Entraining Admixture	905.01
ASTM C-494 Type F High Range Water Reducer	905.02
Synthetic Fibers	ASTM C 1116

Synthetic fibers shall be added at the plant at a rate of three (3) pounds per cubic yard. At the direction of the engineer, Type F high range water reducing (HRWR) admixture may be used. However, the slump, achieved with water, shall not exceed three (3) inches before the HRWR admixture is added to the mix. The HRWR admixture is added to the mix at the plant to increase the desired workability during placement. Type A and Type D water reducers are prohibited because their combination with Type F water reducers cause undesired retardation. Admixtures shall be incorporated into the concrete mix in accordance with the manufacturer's recommendations, at the direction of the engineer. Only one addition of HRWR will be permitted at the jobsite, unless otherwise approved by the engineer.



Back Analysed Deflection Data From HWD

Station	Stress (MPa)	Normalised Deflections							Joint Transfer		Pavement Layer Stiffnesses								Criteria
		d1	d2	d3	d4	d5	d6	d7	d1-d2	d2/d1	E1	E2	E3	E4	E5	E6	E7	E8	
		(microns)							%		(MPa)								

3 (feet) Slabs

3,1	1.178	286	262	248	222	154	108	65	24	0.915	18173	1520	76	144	156	168	181	200	A
3,2	1.240	243	217	207	184	128	90	57	27	0.891	13775	1939	190	124	155	188	232	306	A
3,3	1.207	219	197	194	175	123	87	56	22	0.902	42141	1079	165	156	175	193	214	247	A
3,4	1.265	206	190	179	161	110	79	53	16	0.922	32123	1263	210	191	199	207	215	226	A
3,5	1.126	218	193	202	182	128	93	61	25	0.886									A
3,6	1.122	225	203	202	182	130	92	61	22	0.903	45829	832	293	110	143	179	229	318	A
3,7	1.150	176	153	160	144	107	80	52	23	0.872									A
3,8	1.098	212	187	182	161	110	77	47	26	0.880	24061	1425	255	151	182	215	257	326	A
3,9	1.084	205	183	187	169	114	76	47	22	0.893									A
3,10	1.150	277	234	246	211	135	87	51	43	0.844									A
3,11	1.156	360	237	288	246	143	90	56	124	0.657									D
3,12	1.089	272	235	238	212	146	100	60	37	0.865									A
3,13	1.211	238	206	217	197	138	94	55	32	0.866									A
3,14	1.068	261	235	231	204	134	92	58	26	0.899	37848	250	228	166	172	178	184	193	A
3,15	1.080	253	218	234	212	143	98	60	35	0.862									A
3,16	1.144	244	220	214	190	127	89	56	24	0.902	35956	478	220	166	175	183	192	204	A
3,17	1.119	230	196	208	186	130	94	59	34	0.853									A
3,18	1.174	216	184	194	169	109	73	44	32	0.851									A
3,19	1.173	193	165	174	156	106	72	44	28	0.854									A
3,20	1.157	300	256	261	223	126	85	50	44	0.853									A
3,24	1.190	199	172	175	153	104	77	52	27	0.867									A
3,26	1.208	187	163	163	144	106	80	55	24	0.873	28565	1697	500	156	174	191	211	242	A
3,29	1.215	168	141	148	131	94	70	46	27	0.842									A

4 (feet) Slabs

4,1	1.123	265	234	229	201	136	93	57	31	0.882	26133	657	243	126	150	174	205	255	A
4,2	1.082	303	263	265	233	156	106	65	41	0.866									A

Station	Stress (MPa)	Normalised Deflections							Joint Transfer		Pavement Layer Stiffnesses								Criteria
		d1	d2	d3	d4	d5	d6	d7	d1-d2	d2/d1	E1	E2	E3	E4	E5	E6	E7	E8	
		(microns)							%		(MPa)								

Statistical Analysis of 3 (feet) Slabs

Minimum	1.068	168	141	148	131	94	70	44	16	0.657	13775	250	76	110	143	168	181	193	A
15%ile	1.092	195	167	174	154	106	76	47	22	0.852	19351	549	170	128	155	178	186	201	A
Median	1.156	225	197	202	182	127	87	55	27	0.872	32123	1263	220	156	174	188	214	242	A
85%ile	1.199	257	227	232	207	134	93	58	33	0.896	37848	1520	255	166	175	193	229	306	A
Maximum	1.265	360	262	288	246	154	108	65	124	0.922	45829	1939	500	191	199	215	257	326	D
Average	1.157	234	202	207	183	124	86	54	32	0.868	30941	1165	237	152	170	189	213	251	A
StdDevn	0.054	44	32	35	29	16	10	6	21	0.051	10794	560	116	24	17	15	25	52	

Statistical Analysis of 4 (feet) Slabs

Minimum	1.040	163	154	147	133	97	36	40	9	0.720	8033	250	48	63	150	172	194	228	A
15%ile	1.062	208	180	187	167	119	74	46	22	0.791	18893	494	97	101	152	173	201	240	A
Median	1.105	267	230	232	205	141	90	57	35	0.874	30105	661	243	131	156	181	214	255	A
85%ile	1.157	297	260	261	230	148	97	62	50	0.897	44059	943	484	136	198	211	226	266	B
Maximum	1.326	456	403	374	315	181	106	65	104	0.947	67679	953	498	184	207	579	1767	7866	D
Average	1.129	285	242	247	214	137	85	55	43	0.857	35202	693	281	128	173	263	521	1773	B
StdDevn	0.086	93	75	74	57	24	20	9	28	0.069	22246	287	204	43	27	177	697	3406	

Statistical Analysis of 6 (feet) Slabs

Minimum	1.126	198	176	172	150	101	72	39	21	0.647	7258	570	260	117	158	200	234	276	A
15%ile	1.132	221	194	193	169	113	78	43	22	0.766	9282	770	276	126	163	201	237	280	A
Median	1.179	240	214	208	180	124	83	49	28	0.880	14006	1237	313	146	173	204	245	289	A
85%ile	1.196	258	216	219	198	135	88	52	46	0.892	26242	1468	357	167	190	214	258	342	B
Maximum	1.200	390	252	291	242	149	110	67	138	0.911	38477	1698	401	188	206	224	271	394	D
Average	1.169	260	212	217	189	126	86	50	48	0.836	19914	1168	325	150	179	209	250	320	B
StdDevn	0.032	67	25	40	31	17	13	10	45	0.100	16427	567	71	36	25	13	19	65	

Station	Stress (MPa)	Normalised Deflections							Joint Transfer		Pavement Layer Stiffnesses								Criteria
		d1	d2	d3	d4	d5	d6	d7	d1-d2	d2/d1	E1	E2	E3	E4	E5	E6	E7	E8	
		(microns)							%		(MPa)								
4,3	1.070	278	251	249	222	149	99	63	28	0.901	44059	250	130	131	156	181	214	266	A
4,4	1.086	265	226	235	208	146	103	65	39	0.852									A
4,5	1.130	217	198	190	169	120	88	58	20	0.909	30105	943	484	136	154	172	194	228	A
4,6	1.208	163	154	147	133	97	73	48	9	0.947	67679	953	498	184	198	211	226	248	A
4,11	1.057	456	403	374	315	181	93	58	53	0.884	8033	661	48	63	207	579	1767	7866	B
4,12	1.326	268	193	227	194	121	77	45	75	0.720									B
4,14	1.040	430	326	366	298	145	36	40	104	0.759									D
4,16	1.166	202	172	185	167	119	86	54	30	0.852									A

6 (feet) Slabs

6,1	1.134	243	217	222	203	149	110	67	26	0.893									A
6,2	1.199	229	200	206	182	127	90	53	29	0.872									A
6,3	1.200	237	216	200	176	121	84	49	21	0.911	14006	1698	260	117	158	204	271	394	A
6,11	1.126	263	212	209	178	117	82	49	51	0.806	7258	1237	313	146	173	200	234	289	B
6,12	1.170	198	176	172	150	101	72	44	22	0.888	38477	570	401	188	206	224	245	276	A
6,13	1.187	390	252	291	242	138	80	39	138	0.647									D

Back Analysed Deflection Data From ITX's FWD

Station	Stress (MPa)	Normalised Deflections							Joint Transfer		Pavement Layer Stiffnesses								Criteria
		d1	d2	d3	d4	d5	d6	d7	d1-d2	d2/d1	E1	E2	E3	E4	E5	E6	E7	E8	
		(microns)							%		(MPa)								

3 (feet) Slabs

3,1	0.789	270	240	217	153	105	73	46	30	0.888	9871	250	500	299	300	300	300	301	A
3,2	0.785	240	212	190	132	92	67	43	28	0.885	11085	250	500	386	386	387	387	388	A
3,3	0.781	227	205	182	124	92	64	44	22	0.905	11855	250	500	434	434	435	435	436	A
3,4	0.779	227	200	179	124	88	65	44	28	0.878	11808	250	500	432	432	433	433	434	A
3,5	0.786	222	199	179	126	90	67	44	23	0.895	13438	250	500	415	415	416	416	417	A
3,6	0.792	221	197	178	127	90	65	41	24	0.892	14111	250	500	401	402	402	403	403	A
3,7	0.789	182	157	141	106	79	59	37	25	0.863	19140	250	500	554	554	555	556	556	A
3,8	0.786	214	186	165	110	75	53	33	28	0.871	11515	250	500	547	548	549	549	550	A
3,9	0.79	207	186	166	111	74	53	33	21	0.898	12970	250	500	536	537	537	538	538	A
3,10	0.783	285	241	212	133	87	60	37	44	0.846	5840	250	474	401	401	402	402	403	A
3,11	0.782	325	270	235	131	90	62	39	55	0.832	3876	250	270	548	548	549	550	550	B
3,12	0.776	252	215	189	125	84	60	39	37	0.853	8079	250	500	443	443	444	444	445	A
3,13	0.784	246	221	196	131	89	61	38	24	0.902	9973	250	500	394	394	395	395	396	A
3,14	0.786	241	212	187	121	82	59	37	29	0.881	9048	250	500	464	464	465	465	466	A
3,15	0.777	256	223	197	130	86	62	40	32	0.873	8282	250	500	408	409	409	410	410	A
3,16	0.784	228	198	176	120	84	62	38	30	0.870	10819	250	500	468	468	469	469	470	A
3,17	0.784	222	192	171	121	87	63	38	30	0.864	12052	250	500	456	456	457	457	458	A
3,18	0.785	219	191	169	110	71	49	29	29	0.870	10332	250	500	562	563	563	564	565	A
3,19	0.774	208	175	163	105	73	50	33	34	0.839	11430	250	500	612	612	613	614	615	A
3,20	0.776	311	257	218	127	79	53	33	54	0.826	4203	250	310	533	534	534	535	536	B
3,24	0.786	188	158	141	99	77	58	37	30	0.839	14553	250	500	674	675	676	677	678	A
3,26	0.776	196	169	150	108	82	65	41	27	0.862	15297	250	500	548	549	549	550	551	A
3,29	0.779	175	151	135	97	72	55	34	24	0.862	18044	250	500	675	675	676	677	678	A

Station	Stress (MPa)	Normalised Deflections							Joint Transfer		Pavement Layer Stiffnesses								Criteria
		d1	d2	d3	d4	d5	d6	d7	d1-d2	d2/d1	E1	E2	E3	E4	E5	E6	E7	E8	
		(microns)							%		(MPa)								

4 (feet) Slabs

4,1	0.766	280	244	216	140	93	66	40	36	0.873	6907	250	500	358	359	359	360	360	A
4,2	0.767	324	279	246	155	104	74	41	45	0.862	5070	250	375	329	330	330	330	331	A
4,3	0.783	275	245	216	138	93	67	40	30	0.890	7094	250	500	368	369	369	369	370	A
4,4	0.776	273	244	216	141	99	70	41	30	0.891	7666	250	500	352	353	353	354	354	A
4,5	0.777	223	196	178	126	91	67	41	26	0.883	13399	250	500	411	412	412	413	413	A
4,6	0.779	178	161	147	107	80	60	37	17	0.904	21612	250	500	525	525	526	527	527	A
4,11	0.773	466	381	325	163	90	67	41	85	0.817	2500	250	80	2711	2714	2717	2720	2724	C
4,12	0.777	279	239	208	123	83	60	35	41	0.855	5433	250	450	480	481	481	482	483	A
4,14	0.766	423	327	279	170	69	55	37	96	0.773	2544	250	162	434	435	435	436	436	C
4,16	0.785	226	199	177	125	88	64	37	27	0.882	12366	250	500	424	424	425	425	426	A

6 (feet) Slabs

6,2	0.772	231	198	176	124	89	65	37	34	0.855	11101	250	500	433	434	434	435	435	A
6,3	0.775	251	220	194	133	89	62	34	31	0.878	9380	250	500	387	388	388	389	389	A
6,11	0.776	209	186	165	115	75	53	30	24	0.888	13518	250	500	497	498	498	499	499	A
6,12	0.775	187	165	149	104	71	51	28	22	0.884	16541	250	500	590	591	592	592	593	A
6,13	0.771	285	244	212	135	81	55	29	41	0.857	6303	250	365	429	430	430	431	431	A

Statistical Analysis of 3 (feet) Slabs

Minimum	0.774	175	151	135	97	71	49	29	21	0.826	3876	250	270	299	300	300	300	301	A
15%ile	0.776	199	170	154	106	75	53	33	24	0.841	8140	250	500	401	401	402	402	403	A
Median	0.784	227	199	179	124	84	61	38	29	0.870	11430	250	500	464	464	465	465	466	A
85%ile	0.786	249	218	193	129	90	64	41	31	0.886	13204	250	500	548	549	549	550	551	A
Maximum	0.792	325	270	235	153	105	73	46	55	0.905	19140	250	500	675	675	676	677	678	B
Average	0.783	233	202	180	120	84	60	38	31	0.869	11201	250	481	487	487	488	488	489	A
StdDevn	0.005	38	31	26	13	8	6	4	9	0.023	3782	0	61	96	96	96	96	96	

Station	Stress (MPa)	Normalised Deflections							Joint Transfer		Pavement Layer Stiffnesses								Criteria
		d1	d2	d3	d4	d5	d6	d7	d1-d2	d2/d1	E1	E2	E3	E4	E5	E6	E7	E8	
		(microns)							%		(MPa)								

Statistical Analysis of 4 (feet) Slabs

Minimum	0.766	178	161	147	107	69	55	35	17	0.773	2500	250	80	329	330	330	330	331	A
15%ile	0.766	224	197	177	123	81	60	37	26	0.830	3428	250	237	354	355	355	356	356	A
Median	0.777	277	244	216	139	90	66	40	33	0.877	7001	250	500	418	418	419	419	420	A
85%ile	0.779	313	271	238	152	93	67	41	44	0.888	11191	250	500	469	470	470	471	471	C
Maximum	0.785	466	381	325	170	104	74	41	96	0.904	21612	250	500	2711	2714	2717	2720	2724	D
Average	0.775	295	252	220	139	89	65	39	43	0.863	8459	250	407	639	640	641	642	642	B
StdDevn	0.007	89	65	52	20	10	6	2	26	0.040	5857	0	157	730	731	732	733	734	

Statistical Analysis of 6 (feet) Slabs

Minimum	0.771	187	165	149	104	71	51	28	22	0.855	6303	250	365	387	388	388	389	389	A
15%ile	0.772	200	178	159	110	74	52	29	23	0.856	8149	250	446	412	413	413	414	414	A
Median	0.775	231	198	176	124	81	55	30	31	0.878	11101	250	500	433	434	434	435	435	A
85%ile	0.775	251	220	194	133	89	62	34	34	0.884	13518	250	500	497	498	498	499	499	A
Maximum	0.776	285	244	212	135	89	65	37	41	0.888	16541	250	500	590	591	592	592	593	A
Average	0.774	233	203	179	122	81	57	32	30	0.872	11369	250	473	467	468	468	469	469	A
StdDevn	0.002	38	31	24	13	8	6	4	8	0.015	3907	0	60	79	79	79	79	79	

THE DYNAMIC CONE PENETROMETER

The Dynamic Cone Penetrometer (DCP) is a very robust instrument designed for rapid in-situ measurement of the structural properties of existing road pavements constructed with unbound materials. Continuous measurements can be made down to a depth of 800mm, or further when an extension is fitted. Where pavement layers have different strengths the boundaries can be identified and the thickness of the layers determined. A typical test takes only a few minutes and the instrument therefore provides a very efficient method of obtaining information which would normally require trial pits.

Correlations have been established between measurements with the DCP and California Bearing Ratio (CBR) so that results can be interpreted and compared with CBR specifications for pavement design. Agreement is generally good over most of the range but differences are apparent at low values of CBR, especially for fine grained materials.

The design of the DCP which has been adopted by the Transport Research Laboratory is similar to that described by Kleyn, Maree and Savage (1982) and incorporates an 8kg weight dropping through a height of 575mm and a 60°C cone having a diameter of 20mm. In total it weighs 20kg approx.

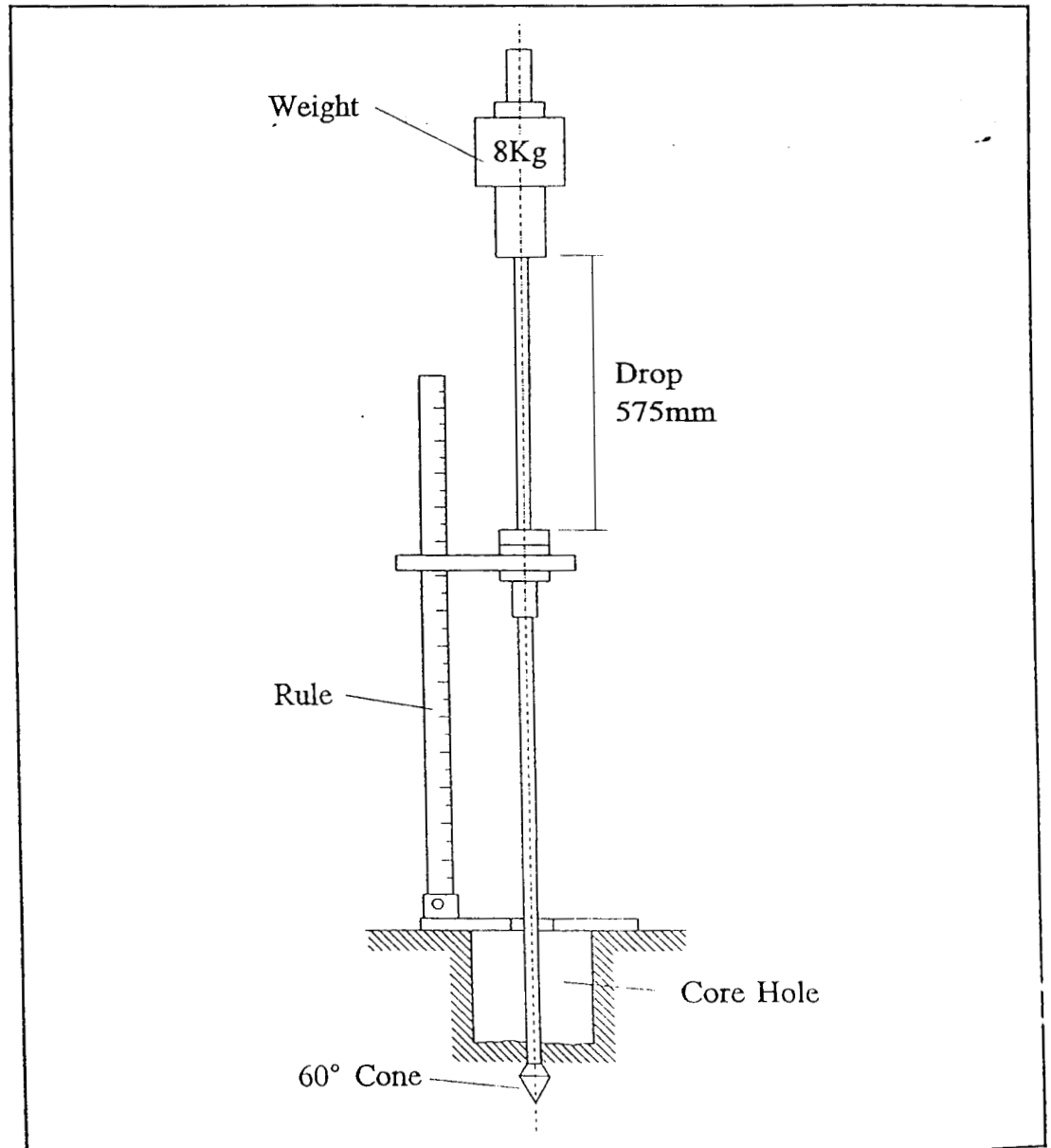
The DCP needs two operators, one to hold the instrument, one to raise and drop the weight. The instrument is held vertically and the weight carefully raised to the handle limit and then allowed to free fall onto the anvil.

It is recommended that a reading should be taken at increments of penetration of about 10mm. However, it is usually easier to take a scale reading after a set number of blows. It is therefore necessary to change the number of blows between readings according to the strength of the layer being penetrated. For good quality granular bases, readings every 5 or 10 blows are satisfactory, but for weaker sub-base layers and subgrades, readings every 1 or 2 blows may be appropriate.

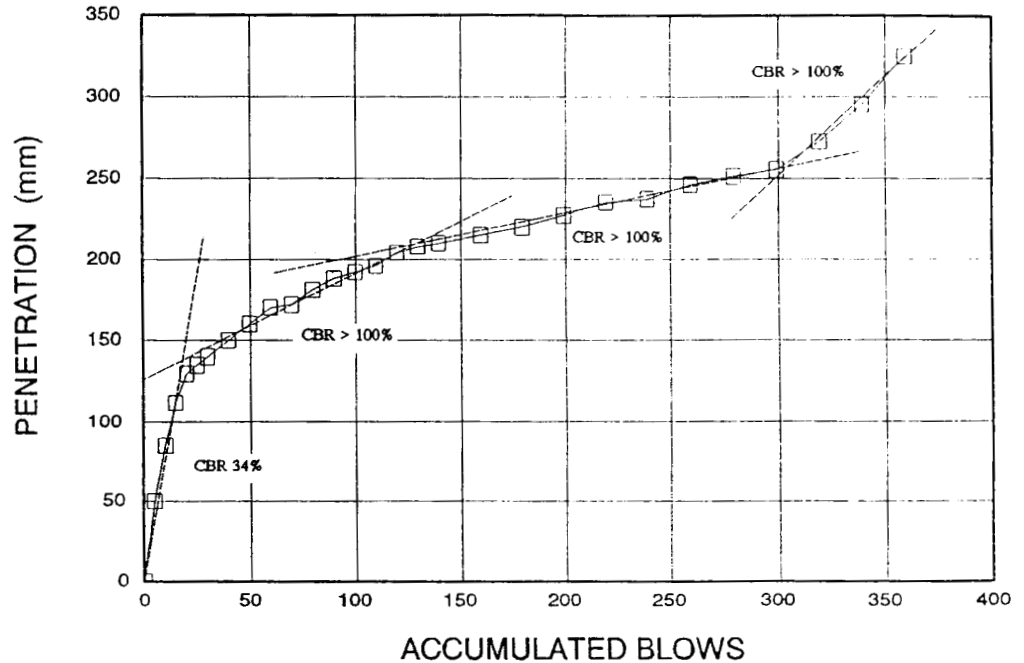
REFERENCE

Kleyn EG, Maree JH and Savage DF (1982), "The application of the pavement DCP to determine the bearing properties and performance of road pavements". Proc. Int. Symp. Bearing Capacity of Roads and Airfields, Trondheim, Norway.

DYNAMIC CONE PENETROMETER (DCP)



DYNAMIC CONE PENETROMETER (DCP) - PENETRATION ν ACCUMULATED BLOWS



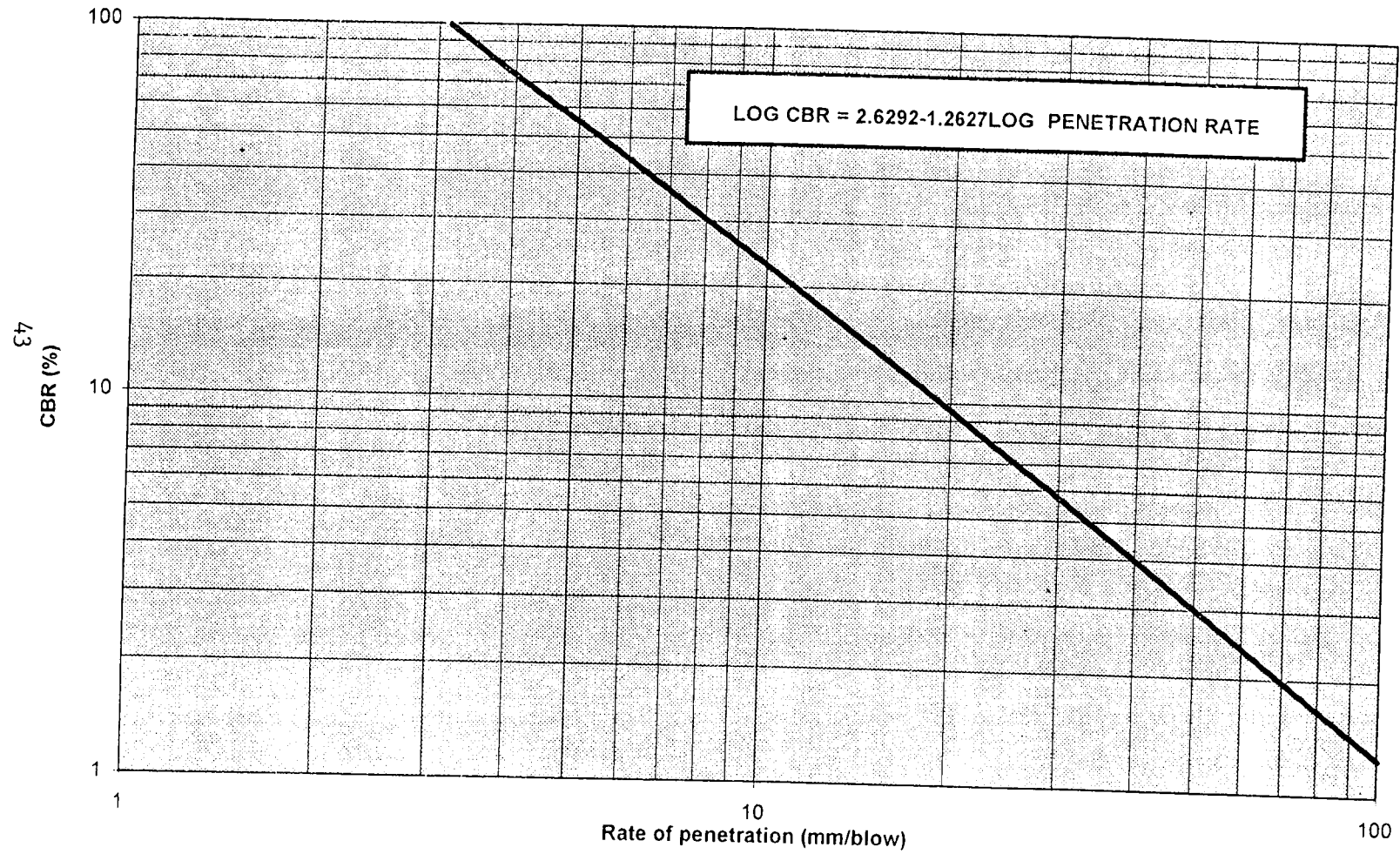
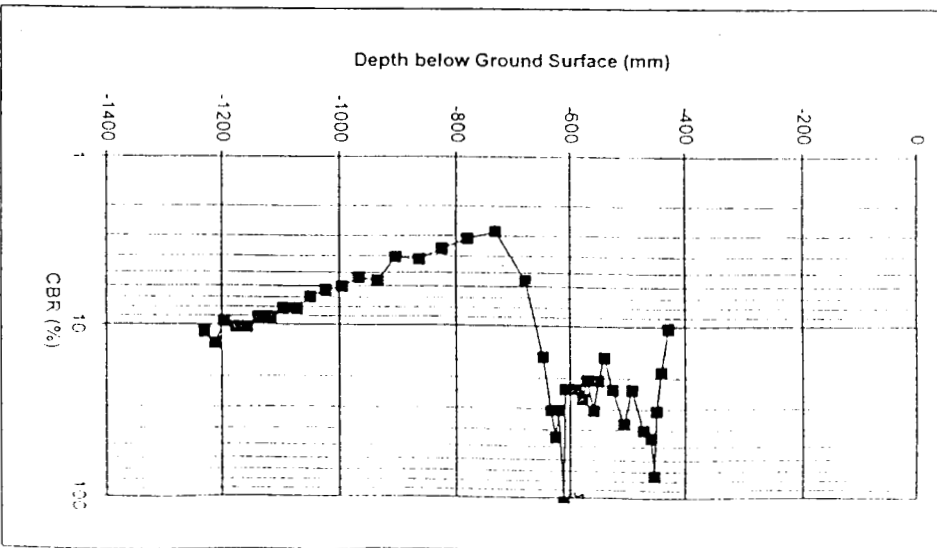
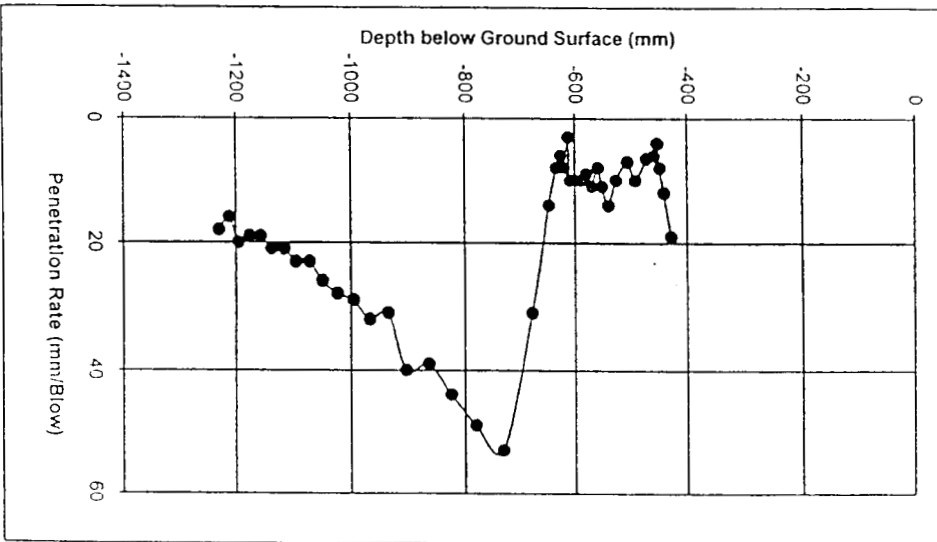
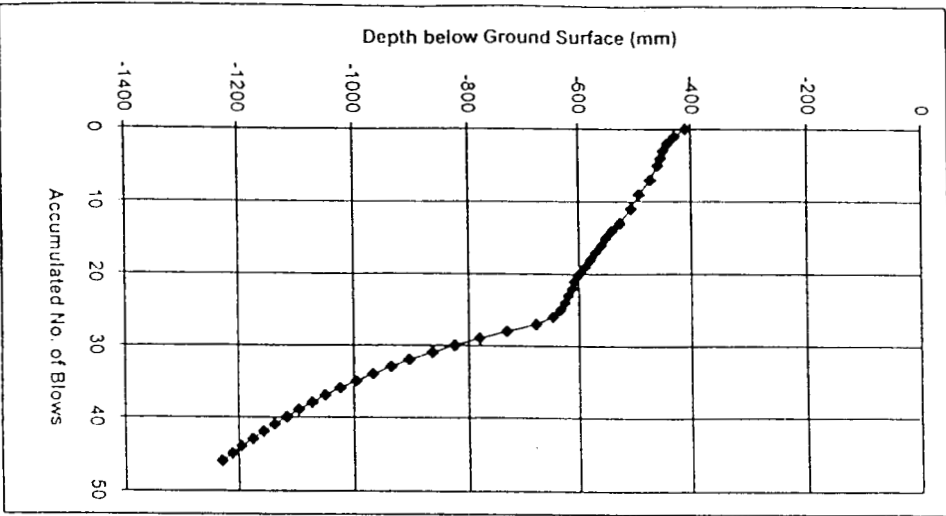
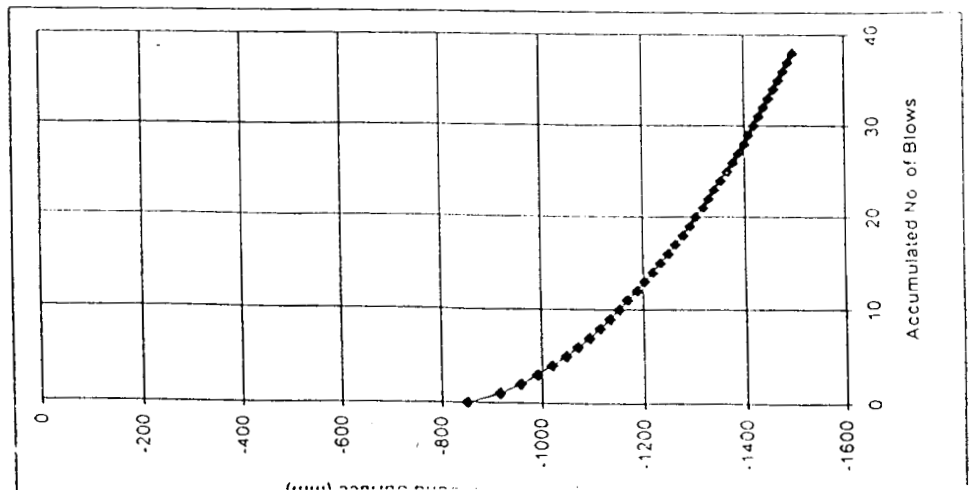
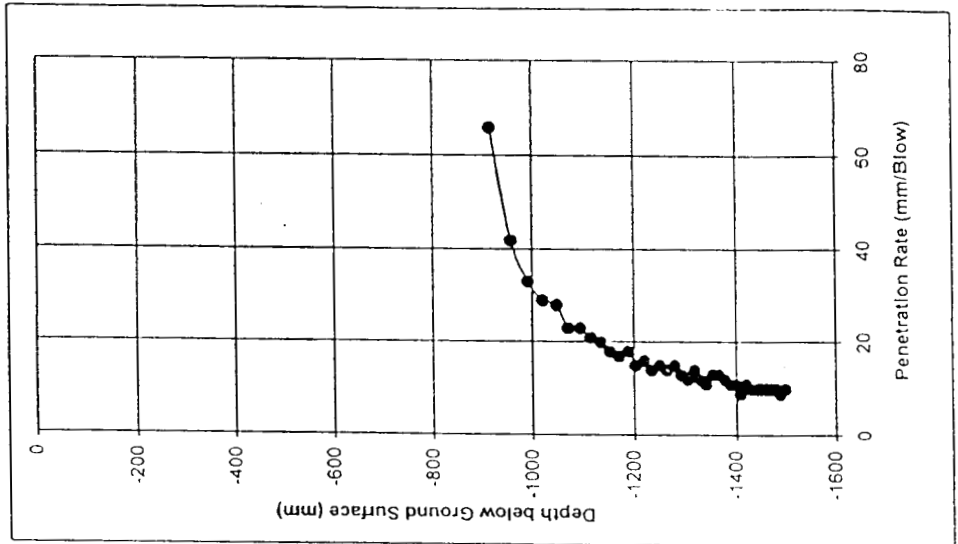
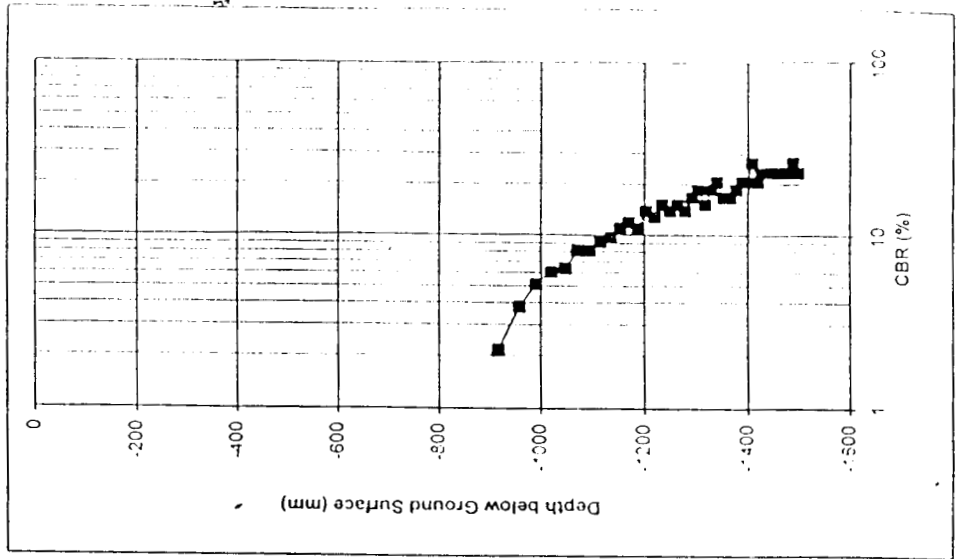


FIGURE 1 : Relationship between DCP penetration rate and CBR value

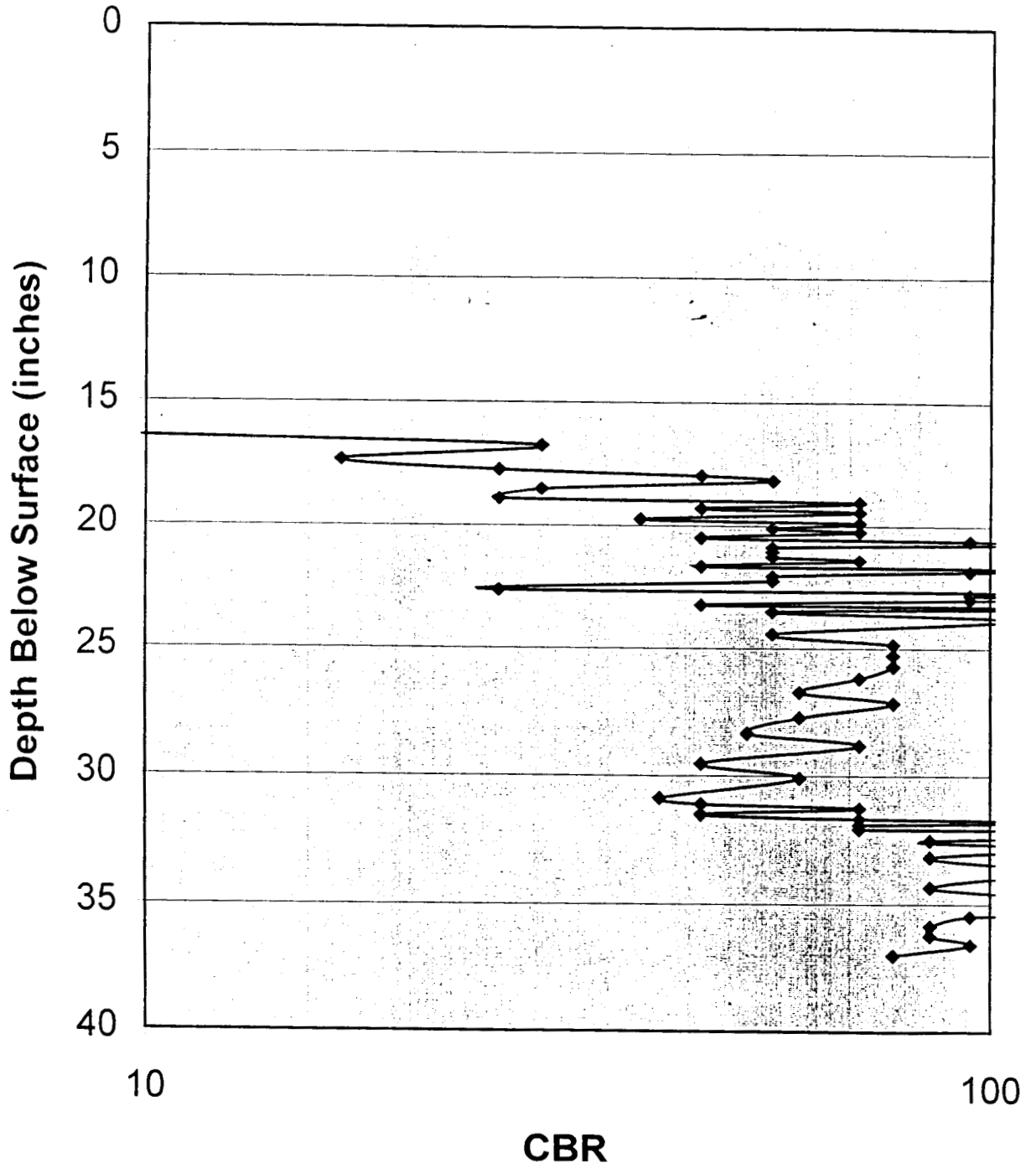
SUMMARY OF DCP TEST RESULTS:



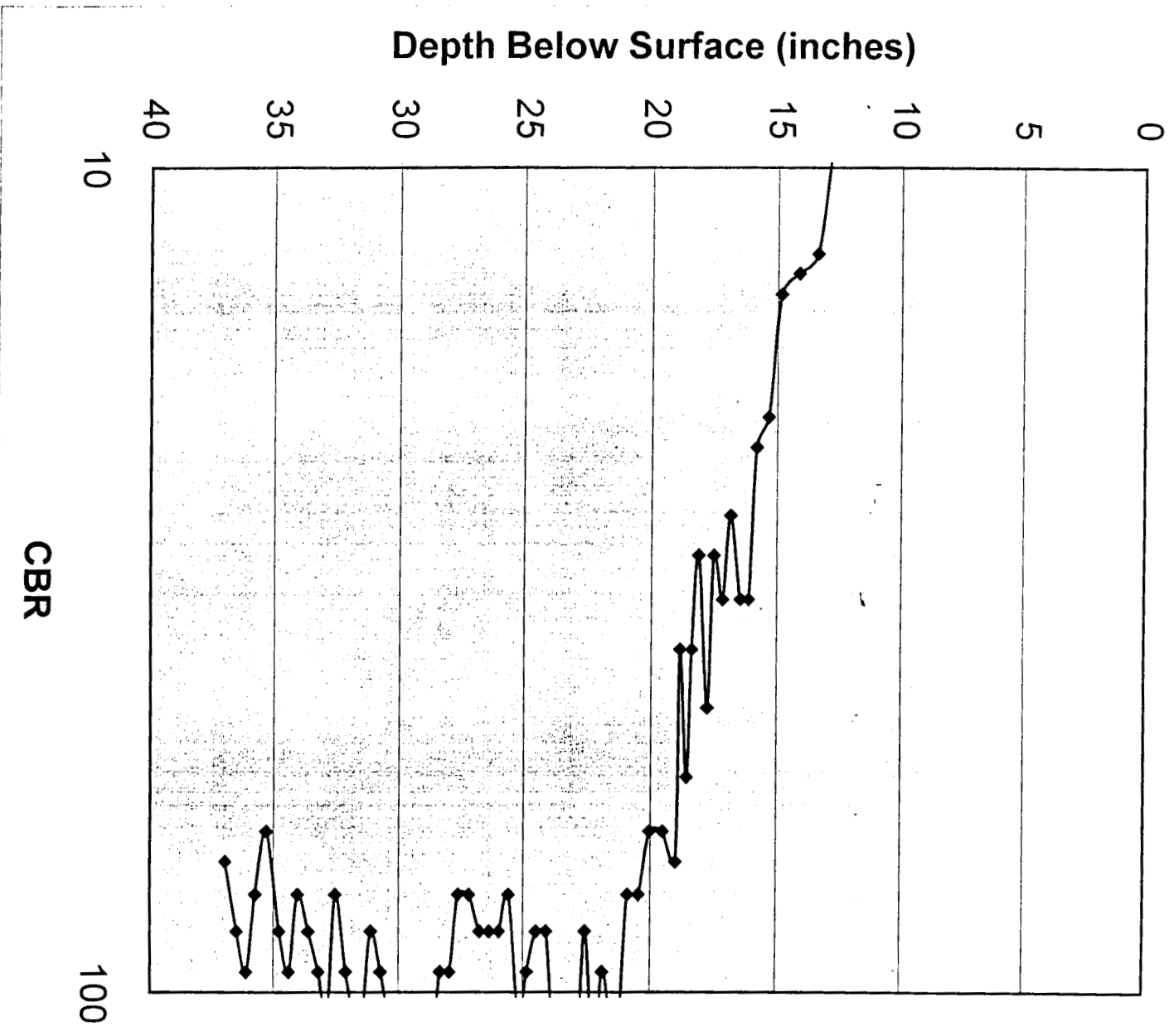
SUMMARY OF DCP TEST RESULTS:



California Bearing Ratio DCP Test at Station 4.11



California Bearing Ratio DCP Test at Station 4.14



APPENDIX G

P (lb)	p (psi)	a (in)	E_A (psi)	c (in)	E_c (psi)	μ	K (pci)	Maximum tensile stress in UTW	
								Eq. 4.7 in Text	CTL Load Test ⁷
5000	43	3.1	1,740,000	3.7	3,400,000	0.150	250	40	43

P (lb)	p (psi)	a (in)	E_A (psi)	c (in)	E_c (psi)	μ	K (pci)	Maximum tensile stress in UTW		Maximum tensile stress in AC	
								Eq. 4.7 in Text	Finite Element	Eq. 4.7 in Text	Finite Element
9000	65	4	1666666	3	3400000	0.15	289	39	45	150	147
9000	65	4	1666666	4	3400000	0.15	289	44	41	118	120
9000	65	4	1666666	5	3400000	0.15	289	44	45	95	96
9000	65	6	1666666	3	3400000	0.15	289	37	36	99	100
9000	65	6	1666666	4	3400000	0.15	289	36	34	82	83
9000	65	6	1666666	5	3400000	0.15	289	34	32	69	68
9000	65	8	1666666	3	3400000	0.15	289	31	31	70	71
9000	65	8	1666666	4	3400000	0.15	289	29	30	60	60
9000	65	8	1666666	5	3400000	0.15	289	27	29	51	50

P (lb)	p (psi)	a (in)	E_A (psi)	c (in)	E_c (psi)	μ	K (pci)	Maximum tensile stress in UTW		Maximum tensile stress in AC	
								Eq. 4.7 in Text	Finite Element	Eq. 4.7 in Text	Finite Element
9000	65	4	1000000	3	3400000	0.15	289	375	394	186	185
9000	65	4	1000000	4	3400000	0.15	289	329	330	133	132
9000	65	4	1000000	5	3400000	0.15	289	289	262	96	93
9000	65	6	1000000	3	3400000	0.15	289	263	250	152	154
9000	65	6	1000000	4	3400000	0.15	289	226	240	117	122
9000	65	6	1000000	5	3400000	0.15	289	199	210	93	93
9000	65	8	1000000	3	3400000	0.15	289	197	170	119	112
9000	65	8	1000000	4	3400000	0.15	289	169	172	95	97
9000	65	8	1000000	5	3400000	0.15	289	148	162	78	80

* Note: All the variables are defined in the text.